THESE

présentée à
l' UNIVERSITE PIERRE ET MARIE CURIE

pour obtenir le titre de

DOCTEUR DE L' UNIVERSITE PARIS 6
spécialité **Mathématiques Appliquées**

par **François DUBOIS**

Sujet de la Thèse :

QUELQUES PROBLEMES LIES AU CALCUL D ' ECOULEMENTS DE FLUIDES PARFAITS DANS LES TUYERES.

Soutenue le 5 janvier 1988 devant le jury composé de

MM.	P.A. RAVIART	Président
	A.Y. LEROUX	
	O. PIRONNEAU	Rapporteurs
	B. MERCIER	
	P. MORICE	
	J.C. NEDELEC	Examinateurs

BOUNDARY CONDITIONS AND THE OSHER SCHEME FOR THE EULER EQUATIONS OF GAS DYNAMICS

François DUBOIS*

September 1987

* Ecole Polytechnique
Centre de Mathématiques Appliquées
91128 PALAISEAU Cedex - France

ABSTRACT

We propose a generalized definition of the multivalued solution of the Riemann problem for hyperbolic conservation laws. It allows a simple presentation of the Osher numerical scheme and a natural treatment of physically relevant boundary conditions for the Euler equations of inviscid compressible fluids. A linearized implicit scheme is derived. Numerical results on shock tube and quasimonodimensional nozzles are presented, showing the attractive convergence properties of the schemes in strong non-linear situations and the adequate coupling of initial and boundary conditions realized by our formulation.

INTRODUCTION

For the numerical resolution of first order systems of conservation laws, the importance of solving the Riemann problem was first recognized by GODUNOV [18]. In recent years, Godunov-type numerical schemes and upstream schemes have been expanded (e.g. HARTEN-LAX-VAN LEER [26]). In particular OSHER [34] proposed a regular (^{1} class) numerical flux which extends to systems the ENGQUIST-OSHER [15,16] scheme. On the other hand the boundary conditions for conservation laws have been analized thanks to the resolution of Riemann problems by DUBOIS-LE FLOCH [10,11].

In this paper we solve the Riemann problem with the use of multivalued rarefaction waves (Section I) and we apply this resolution to construct Godunov-type numerical fluxes that take into account internal interfaces as well as boundary faces. We derive in Section II a compact presentation of the Osher scheme and, in Section III, the treatment of physically relevant boundary conditions for the Euler equations of gas dynamics. Monodimensional test cases involving a first order explicit version of the scheme are presented in Section IV. Section V describes some results for a linearized implicit version of the scheme.

I - MULTIVALUED SOLUTION OF THE RIEMANN PROBLEM

1 - BACKGROUND

We consider an hyperbolic system of conservation laws in one space dimension :

$$\frac{\partial u}{\partial t} + \frac{\partial}{\partial x} f(u) = 0 \tag{1.1}$$

with $u(x,t)$ belonging to a phase space $\mathscr{U} \subset \mathbb{R}^n$ and a regular flux function f $(f : \mathscr{U} \to \mathbb{R}^n)$ whose jacobian $A(u) \equiv df(u)$ admits n real eigenvalues $\lambda_k(u)$:

$$\lambda_1(u) < \lambda_2(u) < \ldots < \lambda_n(u) \quad , \quad u \in \mathscr{U} \ . \tag{1.2}$$

The corresponding eigenvectors are denoted by $r_1(u), r_2(u), \ldots, r_n(u)$. We define a *k-curve* in the phase space $\mathscr{U}$ as a solution of the ordinary differential equation

$$\frac{du}{ds} = r_k(u(s)) \quad , \quad s \in \mathbb{R} \tag{1.3}$$

and we assume that $\mathscr{U}$ is an open set small enough to ensure, for each choice of the initial data

$$u(s_0) = v \quad , \quad v \in \mathscr{U} \quad , \quad s_0 \in \mathbb{R} \tag{1.4}$$

that there is a unique solution $W_k(s;s_0,v)$ to the Cauchy problem (1.3) (1.4). We denote by $\mathscr{W}_k(u_0)$ the k-curve containing u_0. We assume that each k-field is either genuinely non-linear or linearly degenerated. In the former case, the eigenvectors follow

(1.5) $\quad d\lambda_k(u) \cdot r_k(u) \equiv 1$

whereas in the latter case, they satisfy

(1.6) $\quad d\lambda_k(u) \cdot r_k(u) \equiv 0$.

For more details, see LAX [29] or SMOLLER [41].

2 - SIMPLE WAVES

Given a state u_0 in $\mathcal{U}$, the k-curves allow us to build simple waves that classically correspond to rarefactions. Shock waves and contact discontinuities are other selfsimilar (weak) solutions of the conservation law (1.1). In what follows, we will consider a different family of waves : rarefactions, compression waves, and contact discontinuities.

(i) Rarefaction waves

The rarefaction waves are obtained when we look for self-similar solutions of (1.1), that is

(1.7) $\quad u(x,t) = v(\xi) \quad , \quad \xi = \frac{x}{t}$

Then $v(\xi)$ is either a constant state or an eigenvector of $A(v(\xi))$; thus in the following let k be an integer corresponding to a genuinely nonlinear field and we have clearly :

(1.8) $\quad \frac{dv(\xi)}{d\xi} = r_k(v(\xi))$.

Given the value of v in a particular ξ-direction :

(1.9) $\quad v(\xi_0) = u_0$

we have from (1.8) :

(1.10) $\quad v(\xi) = W_k(\xi;\xi_0,u_0)$.

Moreover we also have a constraint on the eigenvalue λ_k :

(1.11) $\quad \lambda_k(v(\xi)) \equiv \xi$.

REMARK 1.1

The condition (1.5) implies that λ_k is increasing along the curve $\mathscr{W}_k$ orientated by the vector r_k. Therefore, the mapping $\xi \mapsto \lambda_k(v(\xi))$ is always non-decreasing along a k-rarefaction wave.

As is well-known, a k-rarefaction is a weak solution of (1.1) satisfying (1.7) and we have (Figure 1.1) :

(1.12)
$$\begin{cases} v(\xi) = u_0 & \xi \leqslant \xi_0 \\ v(\xi) = W_k(\xi;\xi_0,u_0) & \xi_0 \leqslant \xi \leqslant \xi_1 \\ v(\xi) = u_1 & \xi \geqslant \xi_1 \end{cases}$$

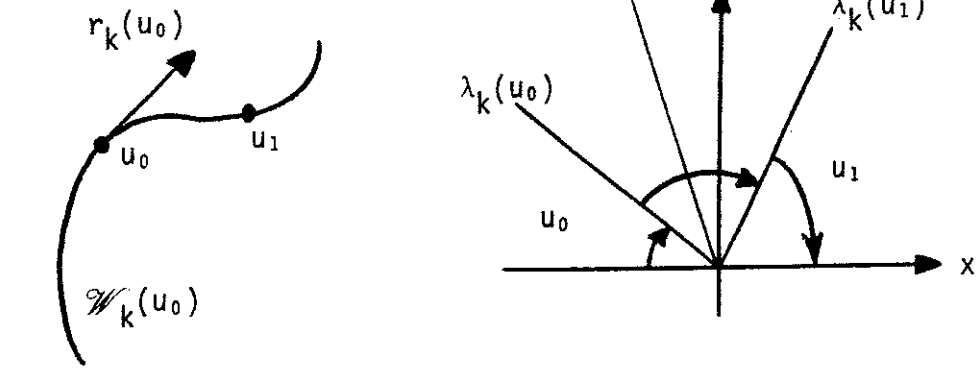

phase space $\qquad$ (x,t) space

Figure 1.1 k-rarefaction wave

(ii) Compression wave or multivalued rarefaction

We claim that Remark 1.1 naturally introduces the necessity of waves other than rarefactions : the classical shock waves. Given u_0 in $\mathcal{U}$, each k-shock wave allows the exploration of a curve in the phase space starting at u_0 with the same two first derivatives as $\mathcal{W}_k(u_0)$ (e.g. LAX [29]). In this section we give a way to explore the k-curve along the direction opposite to r_k.

DEFINITION 1.1

We assume that the k^0 *field is genuinely non-linear. Given states* u_0 *and* u_1 *on the* k*-curve* $\mathcal{W}_k(u_0)$ *satisfying*

$$\lambda_k(u_1) = \xi_1 < \xi_0 = \lambda_k(u_0) \tag{1.13}$$

a k*-compression wave is a continuous function*

$$\mathbf{R} \ni \theta \mapsto (\xi(\theta), w(\theta)) \in \mathbf{R} \times \mathcal{U} \tag{1.14}$$

verifying

$$\begin{cases} \dfrac{d\xi(\theta)}{d\theta} = 1 & \theta < \theta_1 \ , \ \theta > \theta_1' \\ \dfrac{d\xi(\theta)}{d\theta} = -1 & \theta_1 < \theta < \theta_1' \end{cases} \tag{1.15}$$

$$\begin{cases} w(\theta) = u_0 & \theta \leqslant \theta_1 \\ w(\theta) = W_k(\theta;\theta_1,u_0) & \theta_1 \leqslant \theta \leqslant \theta_1' \\ w(\theta) = u_1 & \theta \geqslant \theta_1' \end{cases} \tag{1.16}$$

for some ad hoc real parameters θ_1, θ_1' *(Figure 1.2).*

We set

$$wm(\xi) = \left\{ w(\theta) \,/\, \xi(\theta) = \xi \right\} \ . \tag{1.17}$$

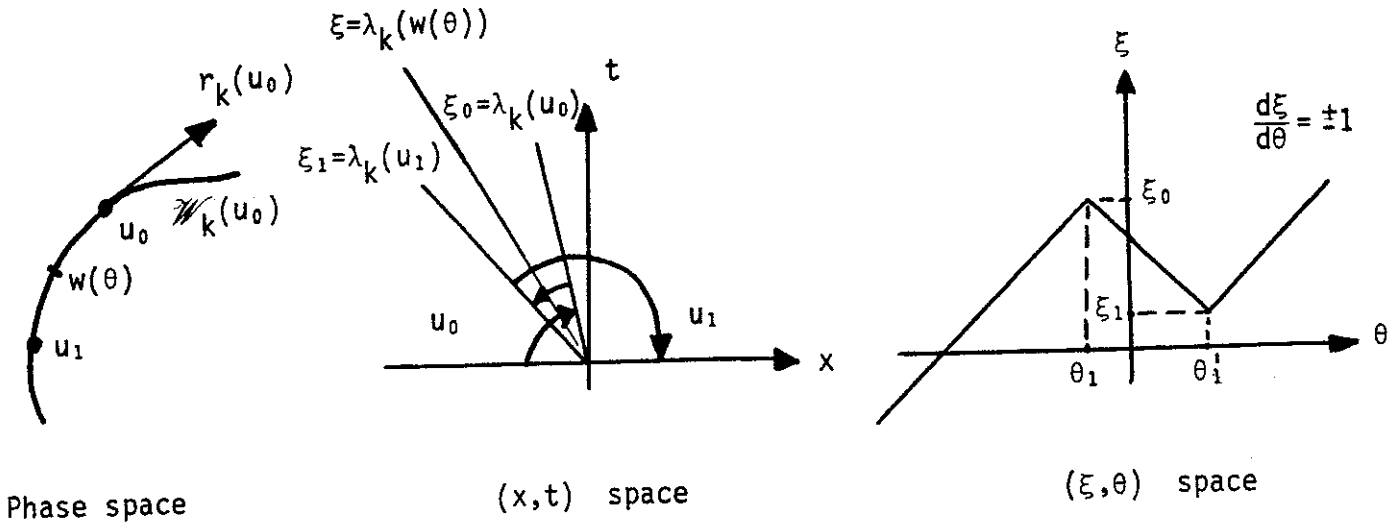

Figure 1.2 k-compression wave (multivalued rarefaction)

REMARK 1.2

We will also speak of a multivalued rarefaction : on the one hand, Definition 1.1 only needs the curve $\mathscr{W}_k(u_0)$, which is classically called the k-rarefaction curve and, on the other hand, the set $wm(\xi)$ is a subset of $\mathscr{U}$ which contains one or three elements. WHITHAM first proposed in [49] such multivalued solutions of conservation laws, as well as their averaging in a shock fitting procedure following the old idea of Maxwell in the context of phase transitions in a Van der Waals gas (e.g. HUANG [28]). The transport-collapse method proposed in [4] by BRENIER is a shock capturing way to average multivalued solutions of scalar conservation laws, which can be extended to systems [5].

(iii) Contact discontinuity

We now assume that the k^0 field is linearly degenerated. We define the k-contact as a multivalued wave in the following sense :

DEFINITION 1.2

We suppose that the k^0 *field is linearly degenerated. Given* u_0 *in* $\mathcal{U}$ *and* u_1 *on the* k*-curve issued from* u_0, *a* k*-contact discontinuity is a continuous function*

$$\mathbb{R} \ni \theta \mapsto (\xi(\theta), w(\theta)) \in \mathbb{R} \times \mathcal{U} \tag{1.18}$$

such that

$$\begin{cases} \dfrac{d\xi(\theta)}{d\theta} = 1 & \theta < \theta_1 \ , \ \theta > \theta_1' \\ \dfrac{d\xi(\theta)}{d\theta} = 0 & \theta_1 < \theta < \theta_1' \end{cases} \tag{1.19}$$

$$\begin{cases} w(\theta) = u_0 & \theta \leqslant \theta_1 \\ w(\theta) = W_k(\theta;\theta_1,u_0) & \theta_1 \leqslant \theta \leqslant \theta_1' \\ w(\theta) = u_1 & \theta \geqslant \theta_1' \end{cases} \tag{1.20}$$

for ad hoc parameters θ_1, θ_1'. *The set* $wm(\xi)$ *is also defined by* (1.17).

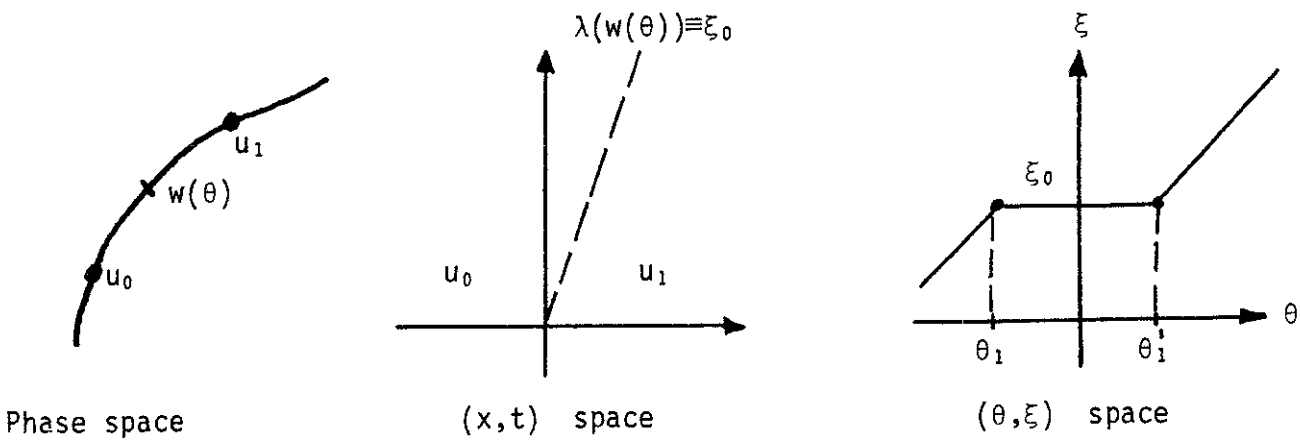

Figure 1.3 k-contact discontinuity

REMARK 1.3

The contact discontinuity is then seen as a multivalued wave of constant eigenvalue in the (x,t) space between the states u_0 and u_1 (Figure 1.3) and the multivalued function $wm(\xi)$ contains a compact interval for $\xi = \lambda_k(u_0)$. Moreover, the above Definitions 1.1 and 1.2 can obviously be extended to the case (i) of rarefaction waves by taking $\xi(\theta) \equiv \theta$.

In the following, we will speak of k-multivalued waves or k-waves when considering one of the three waves defined in the above section.

3 - THE RIEMANN PROBLEM

We now focus on the Riemann problem, the basic Cauchy problem in the theory of hyperbolic conservation laws :

$$R(u_L,u_R)\begin{cases} \dfrac{\partial w}{\partial t} + \dfrac{\partial f(w)}{\partial x} = 0 \quad , \quad w(x,t) \in \mathscr{U} \, , \; x \in \mathbb{R} \, , \; t > 0 \\ w(X,0) = \begin{cases} u_L & x < 0 \\ u_R & x > 0 \end{cases} \end{cases}$$

depending on u_L,u_R in $\mathscr{U}$. With the asumptions on the $\mathscr{W}_k$ curves reviewed in Section 1, the Riemann problem can be solved by (at most) n waves separated by (n-1) constant states in the following sense :

PROPOSITION AND DEFINITION 1.1

1) Let u_L,u_R be given in $\mathscr{U}$ such that $|u_L - u_R|$ is sufficiently small. There exists a unique family of states $u_L \equiv u_0,u_1,\ldots,u_{n-1},u_n \equiv u_R$ satisfying

(1.21) $\quad u_{k+1} \in \mathscr{W}_{k+1}(u_k) \quad ; \quad k = 0,1,\ldots,n-1 \quad .$

2) The multivalued solution of $R(u_L,u_R)$ *is then a continuous function* $\mathbb{R} \ni \theta \mapsto (\xi(\theta), w(\theta)) \in \mathbb{R} \times \mathscr{U}$ *obtained by joining together the constant states* u_j $(j = 0,\ldots,n)$ *by* k*-waves between the states* u_k *and* u_{k+1}, *precisely by :*

$$(1.22) \quad \begin{cases} \theta_1 \leqslant \theta_1' \leqslant \ldots \leqslant \theta_j \leqslant \theta_j' \leqslant \theta_{j+1} \leqslant \ldots \leqslant \theta_n \leqslant \theta_n' \\ \xi(\theta_j) = \lambda_j(u_{j-1}) \qquad j = 1,\ldots,n \\ \xi(\theta_j') = \lambda_j(u_j) \qquad j = 1,\ldots,n \\ \dfrac{d\xi(\theta)}{d\theta} \in \{0,1,-1\} \end{cases}$$

$$(1.23) \quad \begin{cases} w(\theta) = u_L & \theta \leqslant \theta_1 \\ w(\theta) = W_j(\theta;\theta_j,u_{j-1}) & \theta_j \leqslant \theta \leqslant \theta_j' \ , \ j = 1,\ldots,n \\ w(\theta) = u_j & \theta_j' \leqslant \theta \leqslant \theta_{j+1} \ , \ j = 1,\ldots,n-1 \\ w(\theta) = u_R & \theta \geqslant \theta_n' \quad . \end{cases}$$

When θ varies between θ_j and θ_j', the branch of solution is a k wave running from u_{j-1} to u_j and $\xi(\theta)$ is the corresponding eigenvalue which varies from $\lambda_j(u_{j-1})$ to $\lambda_j(u_j)$. The constant state u_j is described by the parameters θ between θ_j' and θ_{j+1} and the function $\xi(\theta)$ varies from $\lambda_j(u_j)$ to $\lambda_{j+1}(u_j)$ (then $\frac{d\xi}{d\theta} = 1$).

REMARK 1.4

The idea of solving the Riemann problem in terms of (eventually) multivalued functions was proposed by VAN LEER [45] for the Burgers' equation. The above definitions rigourously precise what a multivalued wave is in the case of systems.

PROOF OF PROPOSITION 1.1

It is similar to the classical proof of existence (LAX [29]) for the usual Riemann problem ; we mention it briefly. We consider the mapping ϕ defined inductively on a neighbourhood of 0 in $\mathbb{R}^n$ as follows :

$$(\varepsilon_1,\dots,\varepsilon_n) = \varepsilon \mapsto \phi(\varepsilon) = W_n\Big(\varepsilon_n;0,W_{n-1}(\varepsilon_{n-1};0,\dots),W_1(\varepsilon_1;0,u_L)\dots\Big)$$

We obtain easily :

$$\phi(0) = u_L \quad , \quad d\phi(0) = (r_1(u_L),\dots,r_n(u_L))$$

Then the implicit function theorem ensures that a (sub) neighbourhood of 0 is diffeomorphic onto a neighbourhood of u_L. If we set

$$u_k = \phi(\varepsilon_1,\dots,\varepsilon_k,0,\dots,0)$$

then the family $u_k (k = 0,\dots,n)$ solves (1.21).
Moreover, for k-genuinely non-linear waves, we have

$$\varepsilon_k = \lambda_k(u_k) - \lambda_k(u_{k-1}) \tag{1.24}$$

■

REMARK 1.5

An other path which links u_L to u_R begins with the n^0 wave and goes backwards, as proposed by OSHER-SOLOMON [35]. The relations (1.21) are replaced by

$$u_{k+1} \in \mathscr{W}_{n-k}(u_k) \quad , \quad k = 0,1,\dots,n-1 \tag{1.25}$$

The construction proposed in (1.22).(1.23) can be extended in a straightforward way.

II - THE OSHER SCHEME AS A SPLITTING SCHEME

1 - GODUNOV-TYPE NUMERICAL SCHEMES

We briefly recall the classical notions on Godunov-type schemes. All details can be found in the review of HARTEN-LAX-VAN LEER [26]. In a finite volume presentation of 3-point schemes, time step Δt and mesh size Δx are given, and the conservative variables $u(x,t)$ are approached by constant states u_j^n in each control volume

$$V_j^n = \left]\left(j - \frac{1}{2}\right)\Delta x\ ,\ \left(j + \frac{1}{2}\right)\Delta x\right[\times \left[n\Delta t\ ,\ (n+1)\Delta t\right[$$

of the (x,t) space (j integer, n non negative integer).

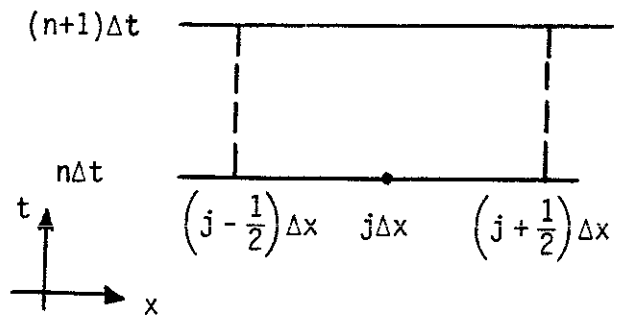

Figure 2.1 Control volume V_j^n in the (x,t) space

The evolution of $\{u_j\}$ is described by :

$$u_j^{n+1} = u_j^n - \frac{\Delta t}{\Delta x}\left(f_{j+\frac{1}{2}}^n - f_{j-\frac{1}{2}}^n\right) \tag{2.1}$$

and the $f_{j+\frac{1}{2}}^n$ are computed with help of the numerical flux function ϕ :

$$f_{j+\frac{1}{2}}^n = \phi\left(u_j^n\ ,\ u_{j+1}^n\right) \quad ,\quad j \text{ integer} . \tag{2.2}$$

The main idea of the Godunov-type schemes is to consider the initial-value problem formed of the partial differential equation (1.1) and the initial-condition

$$(2.3) \qquad u(x,0) = u_j^n \quad , \quad \left(j - \frac{1}{2}\right)\Delta x < x < \left(j + \frac{1}{2}\right)\Delta x$$

Then the integration of (1.1) on the cell V_j^n implies that the value of the function $\phi(u,v)$ is exactly the flux of the solution of the Riemann problem $R(u,v)$ along the axis $t = 0$. In the fundamental example due to GODUNOV [18], $R(u,v)$ is solved exactly, but approached solvers have been developed and studied by ROE [39], HARTEN-LAX [25], VILA [47], DUKOWICZ [12], BRENIER-OSHER [6] among others. Another way to compute the numerical flux is to split algebraically the physical flux between waves of positive speeds coming from the left state u and negative speeds issued from v (STEGER-WARMING [43], VAN LEER [44]). First we find f^+ and f^- satisfying

$$(2.4) \qquad f(u) \equiv f^+(u) + f^-(u) \quad , \quad df^+ \geqslant 0 \ , \ df^- \leqslant 0$$

then the numerical flux satisfies :

$$(2.5) \qquad \phi(u,v) = f^+(u) + f^-(v) \quad .$$

2 - NUMERICAL FLUX OF A MULTIVALUED RIEMANN PROBLEM

According to the ideas recalled previously, the multivalued solution of a Riemann problem (Section I) leads to a numerical scheme if its flux can be defined.

PROPOSITION AND DEFINITION 2.1

We take the notations of Proposition 1.1. The following expression

$$(2.6) \qquad g(\xi;u_L,u_R) = \sum_{\theta \in wm(\xi)} \{f(w(\theta)) - \xi w(\theta)\} \frac{d\xi}{d\theta}(\theta)$$

is defined without ambiguity as a continuous function of the real variable ξ. *We set*

$$(2.7) \qquad \phi(u_L,u_R) = g(0;u_L,u_R) \quad .$$

We can develop the formula (2.7). Let $u_1,\ldots,u_n$ be the intermediate constant states linking $u_0 \equiv u_L$ to $u_n \equiv u_R$ by the k-waves (1.21) and u_k' be the "sonic states" associated to each k-wave :

$$(2.8) \qquad u_k' \in \mathscr{W}_k(u_{k-1}) \quad , \quad \lambda_k(u_k') = 0 \quad , \quad k = 1,\ldots,n \quad .$$

Consider the ε_k $(k = 0,\ldots,n)$ and ε_k' $(k = 1,\ldots,n)$ defined by :

$$(2.9) \qquad \varepsilon_k = \begin{cases} 1 & \text{if } \lambda_k(u_k) \leqslant 0 < \lambda_{k+1}(u_k) \\ 0 & \text{elsewhere} \quad . \end{cases}$$

$$(2.10) \qquad \varepsilon_k' = \begin{cases} 1 & \text{if } \lambda_k(u_{k-1}) \leqslant 0 < \lambda_k(u_k) \\ -1 & \text{if } \lambda_k(u_k) \leqslant 0 < \lambda_k(u_{k-1}) \\ 0 & \text{elsewhere} \quad . \end{cases}$$

with the convention $\lambda_0 \equiv -\infty$, $\lambda_{n+1} \equiv +\infty$. We clearly have

$$(2.11) \qquad \phi(u_L,u_R) = \sum_{k=0}^{n} \varepsilon_k f(u_k) + \sum_{k=1}^{n} \varepsilon_k' f(u_k') \quad .$$

A classic rarefaction is considered to have a positive sign and a backward compression a negative sign, as suggested by Figure 2.2. The contact discontinuity does not give any problem for the evaluation (2.6).(2.7) when located at $\xi = 0$, because the physical flux is constant along this wave.

PROOF OF PROPOSITION 2.1

Figure 2.2 recalls the construction of the multivalued solution of $R(u_0,u_n)$. The arrows follow the continuous function $\xi(\theta)$ whose derivatives are 0 or ± 1. We distinguish between two cases :

(i) $wm(\xi)$ is finite

Thus the only problem comes from the points of discontinuity of $\xi(\theta)$. In that case we set

$$(2.12) \qquad \frac{d\xi}{d\theta} = \frac{1}{2}\left(\frac{d\xi}{d\theta}(\theta^+) + \frac{d\xi}{d\theta}(\theta^-)\right)$$

(ii) $wm(\xi)$ is infinite

Then $wm(\xi)$ contains a branch of rarefaction wave along which $f(w) - \xi w$ is constant and thus ensures the continuity of g towards ξ. ∎

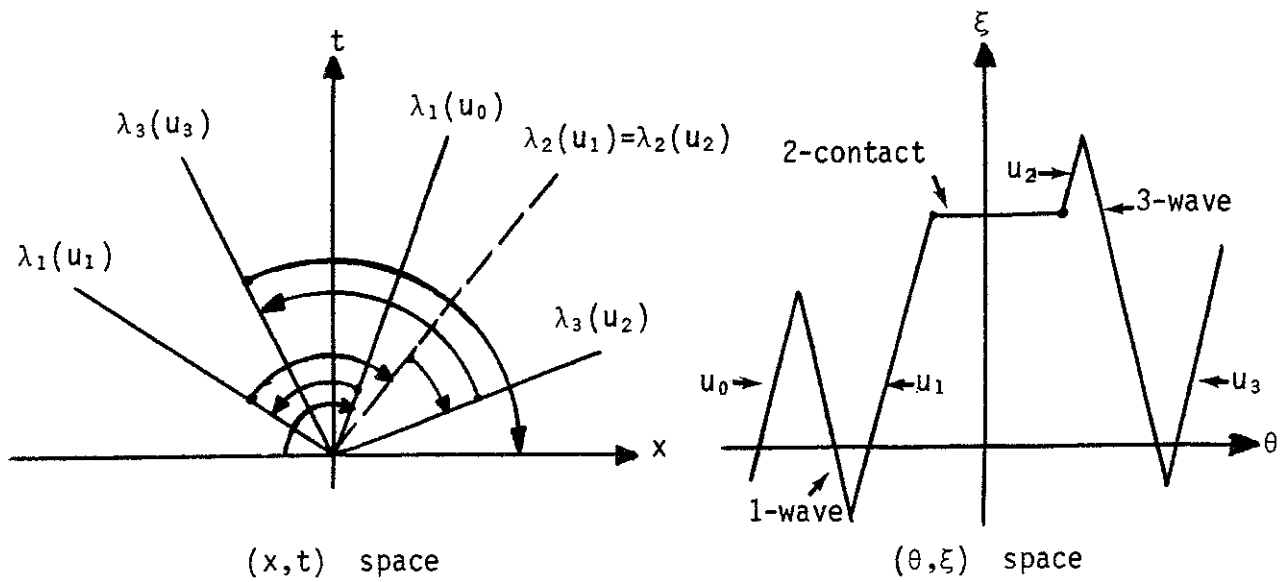

Figure 2.2 Typical wave pattern of a multivalued Riemann problem (Euler equations)

THEOREM 2.1

The numerical flux defined by (2.6)(2.7) *is exactly the* RAI-CHAKRAVARTHY [37] *version of the* Osher *upwind scheme* [34].

REMARK 2.1

A particular version of (2.6)(2.7) was given by VAN LEER [45] in his interpretation of the Engquist-Osher scheme (see also Remark 1.4). Afterwards, the interpretation of the Osher scheme for systems of conservation laws in terms of multivalued solutions of the Riemann problem was pointed out by OSHER himself in [36]: "[the scheme] can be interpreted as solving the incoming Riemann problem in phase space, using only rarefactions, compression, or contact waves, then averaging the resulting multivalued solution as in Godunov's method". The notions established above state precisely this assertion.

REMARK 2.2

In the original version of the Osher scheme, OSHER-SOLOMON [35] proved that the limit solutions satisfy an entropy condition. This scheme corresponds to an unnatural ordering of the waves (see Remark 1.5). However, the natural ordering was used in the numerical experiments of RAI-CHAKRAVARTHY [37]. In the following we only consider this last version of the scheme.

PROOF OF THEOREM 2.1

The numerical flux of the Osher scheme is defined by the union

$$\Gamma = \bigcup_{k=1}^{n} \Gamma_k \tag{2.13}$$

of k-curves, each Γ_k linking u_{k-1} to u_k as a branch of $\mathscr{W}_k(u_{k-1})$, and by the formula

$$(2.14) \qquad \phi(u,v) = \frac{1}{2}\left\{f(u) + f(v) - \int_\Gamma |df(w)|.dw\right\}$$

The definition of the matrices $A^{\pm}(u)$ and $|A(u)|$ is classical : the hypothesis of strict hyperbolicity allows the diagonalization of $A(u) \equiv df(u)$:

$$(2.15) \qquad A(u) \equiv T(u).\Lambda(u).T^{-1}(u)$$

with a diagonal matrix $\Lambda(u)$ of eigenvalues. Given an integer k, the decomposition

$$(2.16) \qquad \lambda_k(u) = \lambda_k^+(u) - \lambda_k^-(u) \qquad , \qquad \lambda_k^{\pm}(u) \geqslant 0$$

allows us to define $\Lambda^{\pm}(u)$ as $\mathrm{Diag}(\lambda_1^{\pm}(u),\ldots,\lambda_n^{\pm}(u))$ and $|\Lambda(u)|$ as $\mathrm{Diag}(\lambda_1^+(u) + \lambda_1^-(u),\ldots,\lambda_n^+(u) + \lambda_n^-(u))$. Then $A^{\pm}(u)$ and $|A(u)|$ correspond to the Λ's as in formula (2.15). We now write (2.14) as

$$(2.17) \qquad \phi(u,v) = f(v) - \int_\Gamma A^+(w).dw \quad .$$

and we prove the theorem in two steps.

- First, we suppose that all the fields are genuinely nonlinear and that each sonic state u_k' defined by (2.8) is in the portion Γ_k of the k-curve. Consider the portion Γ_k' of Γ_k linking u_k' to u_{k+1}' $(k = 1,\ldots,n-1)$ and Γ_0' (resp Γ_n') linking $u_0 \equiv u$ (resp u_n') to u_1' (resp $u_n \equiv v$). We clearly have

$$(2.18) \qquad \phi(u,v) = f(v) - \sum_{k=0}^{n} \int_{\Gamma_k'} A^+(w).dw$$

The computation of each term of this sum is straightforward. Setting $\chi(s)$ for the Heaviside function ($\chi(s) \equiv 1$ if $s > 0$, 0 if $s \leqslant 0$), we have :

$$(2.19)\qquad \phi(u,v) = f(v) - \chi(\lambda_1(u_0))(f(u_1') - f(u_0)) + \\ - \sum_{k=1}^{n-1} \chi(\lambda_k(u_k))(f(u_k) - f(u_k')) + \chi(\lambda_{k+1}(u_k))(f(u_{k+1}') - f(u_k)) \\ - \chi(\lambda_n(u_n))(f(u_n) - f(u_n'))$$

Reordering the terms in (2.19) we get :

$$(2.20)\qquad \phi(u,v) = \sum_{k=0}^{n} \left[\chi(\lambda_{k+1}(u_k)) - \chi(\lambda_k(u_k))\right] f(u_k) \\ + \sum_{k=1}^{n} \left[\chi(\lambda_k(u_k)) - \chi(\lambda_k(u_{k-1}))\right] f(u_k')$$

which is exactly (2.11).

• Let us consider now the general case. The sonic states u_k' may either not exist or be in infinite number (if a k-contact has a null velocity). In the latter case, we simply *choose* a particular state as we have just proposed. If u_k' does not exist on the k-curve $\mathscr{W}_k(u_{k-1})$, we consider an open portion $\tilde{\Gamma}_k$ of $\mathscr{W}_k(u_{k-1})$ containing each compact branch Γ_k defined in (2.13). Then, we introduce an extension $\tilde{\lambda}_k$ of $\lambda_{k|\Gamma_k}$ *different* from $\lambda_{k|\tilde{\Gamma}_k}$ and such that $\tilde{\lambda}_k(u_k') = 0$ for some point u_k' of $\tilde{\Gamma}_k \setminus \Gamma_k$ (see Figure 2.3 for the special case of a k-contact discontinuity). We then introduce the portions of curve Γ_k' exactly as above, and we have

$$(2.21)\qquad \sum_{k=0}^{n} \int_{\Gamma_k'} \tilde{A}^+(w).dw = \int_{\Gamma} A^+(w).dw$$

because the contribution of $\tilde{A}^{+}(w)$ on the portion outside Γ vanishes when we sum the first term of (2.21) (see Figure 2.4). Therefore the computation (2.18)(2.20) in the first step of the proof remains unchanged. ∎

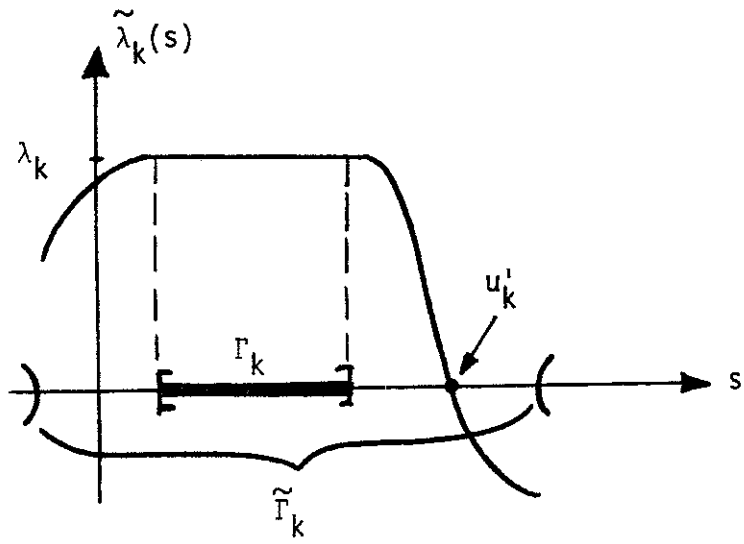

Figure 2.3 Extension $\tilde{\Gamma}_k$ of the curve Γ_k

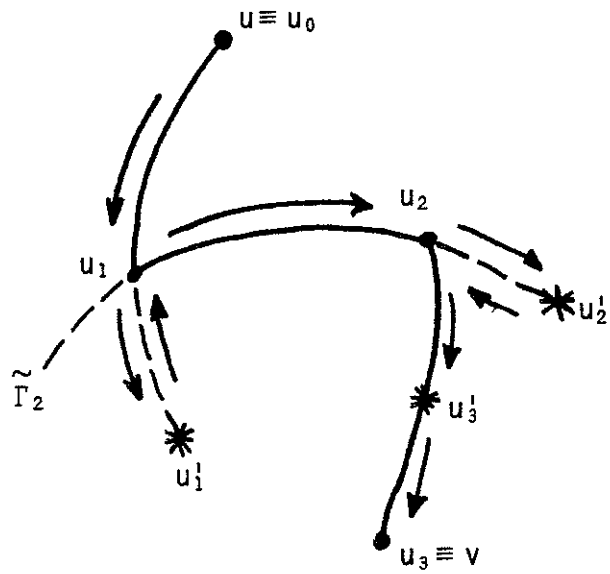

Figure 2.4 Modification of the Osher path of integration

3 - APPLICATION TO THE EULER EQUATIONS OF GAS-DYNAMICS

The Osher scheme can therefore be viewed as a splitting of the numerical flux in terms of some physical fluxes for states involved in the resolution of the multivalued Riemann problem $R(u_L, u_R)$. We detail in this section formulae (2.9)-(2.11) in the particular case of non-isentropic perfect fluids.

From the conservative variables of density, momentum and total energy

$$(2.22) \qquad {}^t U = (\rho, q, \varepsilon) \equiv (\rho, \rho u, \rho E)$$

we compute the pressure p and sound velocity c using

$$(2.23) \qquad E = \frac{u^2}{2} + e \quad , \quad p = (\gamma - 1)\rho e \quad , \quad c^2 = \frac{\gamma p}{\rho}$$

where u, e, γ are respectively the speed, the internal energy and the constant ratio between heat capacities. The physical flux F :

$$(2.24) \qquad {}^t F = (\rho u, \rho u^2 + p\ , \rho u E + p u)$$

is then clearly seen as a function of U if we suppose $\rho > 0$, $\varepsilon > 0$. Moreover the physical entropy will be considered as a variable σ defined by

$$(2.25) \qquad p = \sigma^{2\gamma}\ \rho^{\gamma} \quad .$$

The eigenvalues of $dF(U)$ and the associated Riemann invariants (defined e.g. in SMOLLER [41]) are given by :

	1	2	3
eigenvalue λ	$u-c$	u	$u+c$
Riemann invariants	$\sigma, u+\frac{2c}{\gamma-1}$	u,p	$\sigma, u-\frac{2c}{\gamma-1}$

We now consider the nonstandard nonconservative variables W :

$$(2.26) \qquad {}^tW = (c,u,\sigma)$$

naturally related to the k-curves $\mathscr{W}_k$. In terms of these variables, the physical flux can be evaluated thanks to

$$(2.27) \qquad \rho = \gamma^{-\frac{1}{\gamma-1}} \; c^{\frac{2}{\gamma-1}} \; \sigma^{-\frac{2\gamma}{\gamma-1}}$$

$$(2.28) \qquad p = \gamma^{-\frac{\gamma}{\gamma-1}} \; c^{\frac{2\gamma}{\gamma-1}} \; \sigma^{-\frac{2\gamma}{\gamma-1}} \; .$$

The intermediate states U_1, U_2 (separated by the 2-contact) defined by the relations :

$$(2.29) \qquad \begin{cases} u_1 + \dfrac{2c_1}{\gamma-1} = u_L + \dfrac{2c_L}{\gamma-1} \\ \sigma_1 = \sigma_L \\ u_1 = u_2 \\ p_1 = p_2 \\ u_2 - \dfrac{2c_2}{\gamma-1} = u_R - \dfrac{2c_R}{\gamma-1} \\ \sigma_2 = \sigma_R \end{cases}$$

are given explicitly as :

$$(2.30)\qquad \begin{cases} c_1 = \dfrac{1}{1+\sigma_R/\sigma_L}\left(c_L + \dfrac{\gamma-1}{2}u_L + c_R - \dfrac{\gamma-1}{2}u_R\right) \\ u_1 = u_2 = \dfrac{1}{1+\sigma_L/\sigma_R}\left(\dfrac{2}{\gamma-1}c_L + u_L\right) + \dfrac{1}{1+\sigma_R/\sigma_L}\left(-\dfrac{2}{\gamma-1}c_R + u_R\right) \\ c_2 = \dfrac{1}{1+\sigma_L/\sigma_R}\left(c_L + \dfrac{\gamma-1}{2}u_L + c_R - \dfrac{\gamma-1}{2}u_R\right) \ . \end{cases}$$

Only two sonic points U_1' and U_3' are usefull, and satisfy :

$$(2.31)\qquad \begin{cases} u_1' + \dfrac{2c_1'}{\gamma-1} = u_L + \dfrac{2c_L}{\gamma-1} \\ \sigma_1' = \sigma_L \\ u_1' - c_1' = 0 \end{cases}$$

$$(2.32)\qquad \begin{cases} u_3' - \dfrac{2c_3'}{\gamma-1} = u_R - \dfrac{2c_R}{\gamma-1} \\ \sigma_3' = \sigma_R \\ u_3' + c_3' = 0 \end{cases}$$

Thus, the states U_1, U_2, U_1', U_3' needed for the computation of $\phi(u_L,u_R)$ are easily evaluated in terms of the W-variables (formulae (2.29)-(2.32)). This can be done quickly on a vector-processor. Then the ε-coefficients of formulae (2.9)-(2.10) satisfy :

$$\begin{cases} \varepsilon_L \equiv \varepsilon_0 = \begin{cases} 1 & \text{if } 0 < u_L - c_L \\ 0 & \text{elsewhere} \end{cases} \\ \varepsilon_1' = \begin{cases} 1 & \text{if } u_L - c_L \leqslant 0 < u_1 - c_1 \\ -1 & \text{if } u_1 - c_1 \leqslant 0 < u_L - c_L \\ 0 & \text{elsewhere} \end{cases} \\ \varepsilon_1 = \begin{cases} 1 & \text{if } u_1 - c_1 \leqslant 0 < u_1 \\ 0 & \text{elsewhere} \end{cases} \end{cases}$$

(2.33)
$$\left\{\begin{array}{lll} \varepsilon_2 = \left\{\begin{array}{ll} 1 & \text{if } u_2 \leqslant 0 < u_2 + c_2 \\ 0 & \text{elsewhere} \end{array}\right. \\ \varepsilon_3' = \left\{\begin{array}{ll} 1 & \text{if } u_2 + c_2 \leqslant 0 < u_R + c_R \\ -1 & \text{if } u_R + c_R \leqslant 0 < u_2 + c_2 \\ 0 & \text{elsewhere} \end{array}\right. \\ \varepsilon_R \equiv \varepsilon_3 = \left\{\begin{array}{ll} 1 & \text{if } u_R + c_R \leqslant 0 \\ 0 & \text{elsewhere} \end{array}\right. \end{array}\right.$$

and the evaluation (2.11) of the numerical flux becomes :

(2.34)
$$\phi(u_L, u_R) = \varepsilon_L f(u_L) + \varepsilon_1' f(u_1') + \varepsilon_1 f(u_1) + \\ + \varepsilon_2 f(u_2) + \varepsilon_3' f(u_3') + \varepsilon_R f(u_R) .$$

The relations (2.29)-(2.34) are the only ones necessary to cover all the cases involved in the Osher scheme. We think that this presentation unifies the one usually proposed (e.g. RAI-CHAKRAVARTHY [37]).

III - NUMERICAL BOUNDARY CONDITIONS FOR THE EULER EQUATIONS

1 - GENERALITIES

The numerical treatment of boundary conditions for the Euler equations of inviscid gas dynamics is a question of major importance in external as well as in internal aerodynamics but few rigorous mathematical results have been established. More precisely, the treatment commonly proposed in a majority of computing codes is based on a linearized analysis (characteristics theory, e.g. VIVIAND-VEUILLOT [48], CHAKRAVARTHY [8]). Rigorous results concerning the stability properties of this approach can be found in GUSTAFSSON-KREISS-SUNDSTRÖM [23], OLIGER-SUNDSTRÖM [33], GOLDBERG-TADMOR [20]. Locally nonlinear approaches of initial boundary value problems were also theoretically proposed by LIU [30], NISHIDA-SMOLLER [32], GOODMAN [21]. In [2], BARDOS-LEROUX-NEDELEC presented a non local approach of the problem in the case of scalar conservation laws. This work was extended to systems by DUBOIS-LE FLOCH [11] by the so-called boundary entropy inequality, also proposed by AUDOUNET [1] and MAZET et al [31] with variational arguments. Moreover, in [10], DUBOIS-LE FLOCH proposed a new approach based on the Riemann problem and proved that in linear and (not necessarily convex) scalar cases, this approach is equivalent to the boundary entropy inequality.

On the other hand, the finite volume method leads numerically to a formulation of boundary conditions in terms of a numerical flux at the boundary, as was early recognized by GODUNOV (e.g. Godunov et al [19]) and RIZZI [38]. In this section we derive a *strong nonlinear*

treatment of the boundary condition, i.e. the computation of boundary fluxes with the help of multivalued Riemann problems. We focus on some significant physical examples as proposed in [48,8]. In an external problem, an artificial boundary defines a "numerical infinity" and two numerical conditions are to be examined : the boundary condition at infinity and the sliding on the rigid boundary. In the case of internal problems such as nozzles, four cases must be considered according to inflow or outflow at the boundary and to the magnitude of velocity (subsonic, supersonic). In the following we analyse these cases from a physical point of view :

1) for supersonic inflow we assume that a state is entirely given ;

2) for subsonic inflow the fluid is given by its static thermodynamical properties, e.g. total enthalpy and entropy ;

3) for subsonic outflow static pressure is supposed to be given, and

4) for supersonic outflow no numerical datum is required.

For each of these physical boundary conditions we give a computation of the numerical flux ϕ at the boundary for monodimensional problems. This analysis is valid along the normal of the boundary for multidimensional problems thanks to Galilée invariance of the Euler equations. A state computed at time $n\Delta t$ in the cell number j located along the boundary is denoted by $U_j^n \equiv V = {}^t(\rho,\rho u,\rho E)$ (Figure 3.1)

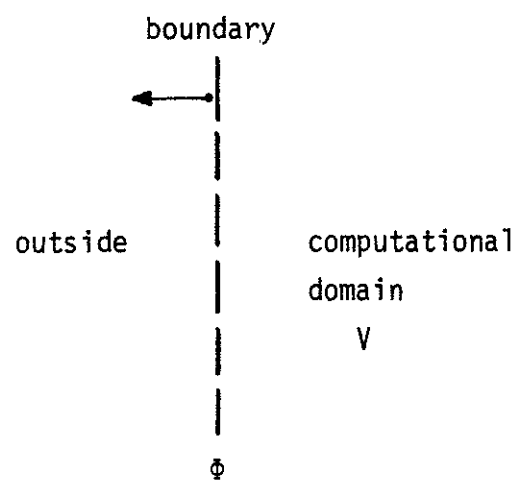

Figure 3.1 Notations

2 - SUPERSONIC INFLOW, BOUNDARY CONDITION AT INFINITY

In this case, a physical state is supposed to be given. Therefore, the analysis of DUBOIS-LE FLOCH [10] can be applied without modification. Suppose, for example, that the computational domain is on the right, and that the given state u_B is on the left. The boundary flux is then computed by

$$\phi = \phi(u_B, V) \tag{3.1}$$

where $\phi(.,.)$ is the Osher flux derived in Section II.

3 - RIGID WALL BOUNDARY CONDITION

The physical boundary condition is

$$u = 0 \quad \text{on the wall} \tag{3.2}$$

(i.e. normal velocity null in the multidimensional case). Then the boundary flux takes the form :

$$\phi = {}^t(0,p,0) \tag{3.3}$$

which can be obtained, in terms of the Riemann problem, by the "mirror state" $\tilde{V}$ of V, defined by

$$\tilde{\rho} = \rho \quad , \quad \tilde{\rho u} = -\rho u \quad , \quad \tilde{\rho E} = \rho E \quad .$$

Thus we have :

$$\phi = \phi(\tilde{V}, V) \tag{3.4}$$

4 - SUBSONIC OUTFLOW

We only consider the case of a given static pressure P. In the usual way, a state is computed on the boundary thanks to the condition $p = P$ and following the two outgoing characteristics from the computational domain, eventually in a nonlinear way (e.g. CHAKRAVARTHY-OSHER [9]). However, we could set this problem in those terms : how to replace u_B in (3.1) ? We prefer to consider the condition on p as a two-dimensional manifold $\mathscr{P}$ in the state space $\mathscr{U} \subset \mathbb{R}^3$. Then a "partial Riemann problem" $R(V, \mathscr{P})$ (the boundary is now on the right of $V \equiv V_L$) can be solved with only a 1-wave issued from V intersecting $\mathscr{P}$ at U_1 (Figure 3.2).

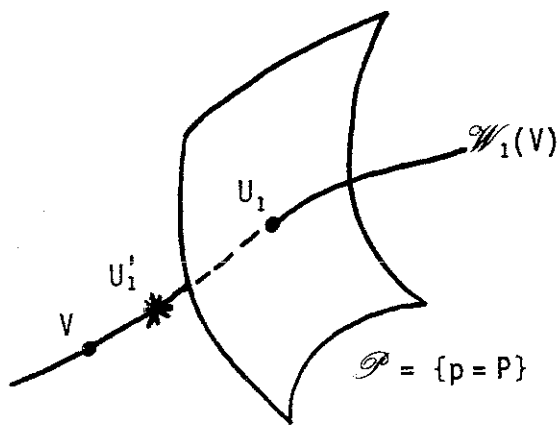

Figure 3.2 Given static pressure on the outflow (phase space)

The computation of this state is easy ; the equations of U_1 are

$$(3.5) \qquad \begin{cases} u_1 + \frac{2}{\gamma-1} c_1 = u_L + \frac{2}{\gamma-1} c_L \\ \sigma_1 = \sigma_L \\ p_1 = P \end{cases}$$

Then we have :

$$(3.6)\qquad \begin{cases} c_1 = \sqrt{\gamma}\ \sigma_L\ p^{\frac{\gamma-1}{2\gamma}} \\ u_1 = u_L + \frac{2}{\gamma-1} c_L - \frac{2}{\gamma-1}\sqrt{\gamma}\ \sigma_L\ p^{\frac{\gamma-1}{2\gamma}} \\ \sigma_1 = \sigma_L \end{cases}$$

and the boundary flux is given by

$$(3.7)\qquad \phi = \varepsilon_L\, f(V_L) + \varepsilon_1'\, f(U_1') + \varepsilon_1\, f(U_1)$$

with the epsilons given by formulae

$$(3.8)\qquad \begin{cases} \varepsilon_L = \begin{cases} 1 & \text{if } 0 < u_L - c_L \\ 0 & \text{elsewhere} \end{cases} \\ \varepsilon_1' = \begin{cases} 1 & \text{if } u_L - c_L \leqslant 0 < u_1 - c_1 \\ -1 & \text{if } u_1 - c_1 \leqslant 0 < u_L - c_L \\ 0 & \text{elsewhere} \end{cases} \\ \varepsilon_1 = \begin{cases} 1 & \text{if } u_1 - c_1 \leqslant 0 \\ 0 & \text{elsewhere} \end{cases} \end{cases}$$

REMARK 3.1

This approach for initial-boundary Riemann problems is already to be found in GODUNOV [19], and VILA [46] proposed it in the particular case of Saint-Venant shallow water equations.

5 - SUBSONIC INFLOW

In this case, total enthalpy and physical entropy are given :

$$(3.9)\qquad \frac{u^2}{2} + \frac{c^2}{\gamma-1} = H \quad , \quad \frac{p^{\frac{1}{2\gamma}}}{\sqrt{\rho}} = \Sigma \quad .$$

These conditions define a curve $\mathscr{HS}$ in the phase space $\mathscr{U}$ which is the left datum for a Riemann problem whose right datum is V (Figure 3.3). The resolution of this problem is given by a state U_1 on $\mathscr{HS}$ followed by U_2 on $\mathscr{W}_2(U_1)$ in such a way that V lies in $\mathscr{W}_3(U_2)$. Algebraically, we have :

$$(3.10)\qquad \begin{cases} \dfrac{u_1^2}{2} + \dfrac{c_1^2}{\gamma-1} = H \\ \sigma_1 = \Sigma \\ u_1 = u_2 \\ p_1 = p_2 \\ u_2 - \dfrac{2}{\gamma-1} c_2 = u_R - \dfrac{2}{\gamma-1} c_R \equiv R_d \\ \sigma_2 = \sigma_R \end{cases}$$

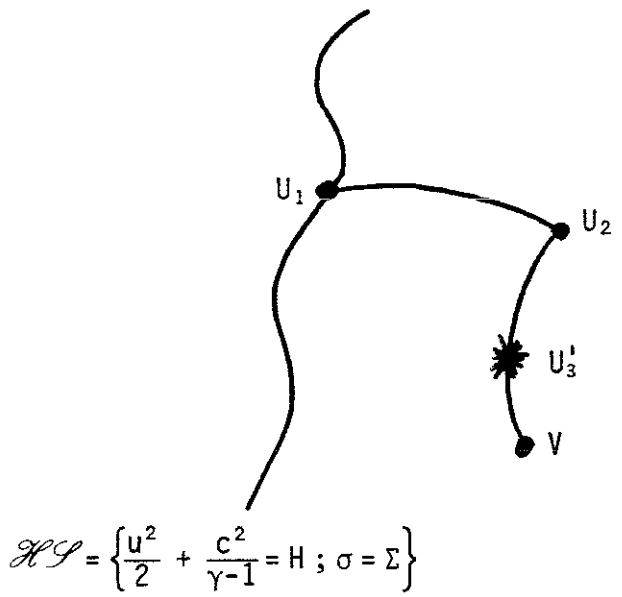

Figure 3.3 Given total enthalpy and physical entropy on the inflow (phase space)

Eliminating u_1, p_1, u_2, p_2, σ_2 from (3.10), we get a polynomial equation of degree 2 for c_1 :

$$\left\{1 + \frac{\gamma-1}{2}\left(\frac{\Sigma}{\sigma_R}\right)^2\right\} c_1^2 - (\gamma-1)\left(\frac{\Sigma}{\sigma_R}\right)^2 R_d c_1 + \tag{3.11}$$
$$+ \left(\frac{\gamma-1}{2}\right)^2 \left(\frac{\Sigma}{\sigma_R}\right)^4 (R_d^2 - 2H) = 0$$

The equation (3.11) has real solutions under the condition

$$\left(u_R - \frac{2}{\gamma-1} c_R\right)^2 \leqslant 2\left(1 + \frac{2}{\gamma-1}\left(\frac{\sigma_R}{\Sigma}\right)^2\right) H \tag{3.12}$$

which can be seen as a cavitation condition. We recall that we need such a condition to be able to solve the Riemann problem in terms of physically acceptable states (i.e. $\rho > 0$, $p > 0$) :

$$u_R - \frac{2}{\gamma-1} c_R \leqslant u_L + \frac{2}{\gamma-1} c_L \quad . \tag{3.13}$$

If $R_d^2 \leqslant 2H$, (3.11) admits only one positive and physically acceptable solution. If

$$2H < R_d^2 \leqslant 2H\left(1 + \frac{2}{\gamma-1}\left(\frac{\sigma_R}{\Sigma}\right)^2\right) \tag{3.14}$$

then the equation (3.11) has two positive solutions, and the state U_1 is outgoing (!). In this case, a subsonic solution is the continuation of the unique physically acceptable solution obtained when $R_d^2 \leqslant 2H$. We also have a new outgoing supersonic solution but this is thrown out. Then under the hypothesis (3.12) the solution of (3.10) is given by

$$(3.15)\qquad \begin{cases} c_1 = \dfrac{\gamma-1}{2}\left(\dfrac{\Sigma}{\sigma_R}\right)^2 (u_1 - R_d) \\ u_1 = \dfrac{\dfrac{\gamma-1}{2}\left(\dfrac{\Sigma}{\sigma_R}\right)^2 R_d + \sqrt{2\left(1+\dfrac{\gamma-1}{2}\left(\dfrac{\Sigma}{\sigma_R}\right)^2\right)H - \dfrac{\gamma-1}{2}\left(\dfrac{\Sigma}{\sigma_R}\right)^2 R_d^2}}{1 + \dfrac{\gamma-1}{2}\left(\dfrac{\Sigma}{\sigma_R}\right)^2} \\ \sigma_1 = \Sigma \end{cases}$$

$$(3.16)\qquad \begin{cases} c_2 = \dfrac{\sigma_d}{\Sigma}\, c_1 \\ u_2 = u_1 \\ \sigma_2 = \sigma_R \end{cases}$$

Those relations replace the computation of U_1 and U_2 by (2.29)(2.30) in the usual case. The formulae (2.32) defining U_3' are unchanged, and no 1-wave exists for the resolution of the problem $R(\mathcal{HS},V)$. We finally have :

$$(3.17)\qquad \phi = \varepsilon_1 f(U_1) + \varepsilon_2 f(U_2) + \varepsilon_3' f(U_3') + \varepsilon_R f(V_R)$$

with

$$(3.18)\qquad \begin{cases} \varepsilon_1 = \begin{cases} 1 & \text{if } 0 < u_1 \\ 0 & \text{elsewhere} \end{cases} \\ \varepsilon_2 = \begin{cases} 1 & \text{if } u_2 \leqslant 0 < u_2 + c_2 \\ 0 & \text{elsewhere} \end{cases} \\ \varepsilon_3' = \begin{cases} 1 & \text{if } u_2 + c_2 \leqslant 0 < u_R + c_R \\ -1 & \text{if } u_R + c_R \leqslant 0 < u_2 + c_2 \\ 0 & \text{elsewhere} \end{cases} \\ \varepsilon_R = \begin{cases} 1 & \text{if } u_R + c_R \leqslant 0 \\ 0 & \text{elsewhere} \end{cases} . \end{cases}$$

6 - SUPERSONIC OUTFLOW

No numerical data are related to this last case. Considering that the initial state V is on the left of the boundary, we must imagine that a state to the right of this boundary forces all the waves to go outside. If V is a supersonic outgoing state (i.e. $u_L - c_L > 0$) this condition is automatically realized. In the other case, a right state with high positive speed will produce a 1-wave which will contribute to the flux of the boundary Riemann problem (Figure 3.4).

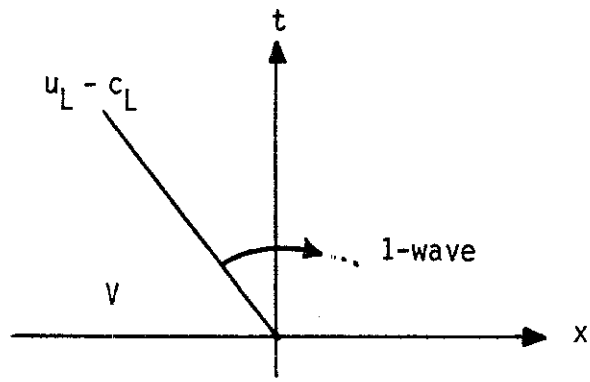

Figure 3.4 Supersonic outflow

Because we have very little information about the right state, we only consider for the Riemann problem this 1-rarefaction wave. Then, the flux is given by

$$\phi = \varepsilon_L f(V_L) + \varepsilon_1' f(U_1') \tag{3.19}$$

with U_1' computed thanks to (2.31) and with the epsilons verifying

$$(3.20)\qquad \begin{cases} \varepsilon_L = \begin{cases} 1 & \text{if } 0 < u_L - c_L \\ 0 & \text{elsewhere} \end{cases} \\ \varepsilon_1' = \begin{cases} 1 & \text{if } u_L - c_L \leqslant 0 \\ 0 & \text{elsewhere} \end{cases} \end{cases}$$

7 - CONCLUSION

All the numerical boundary conditions developed in Sections 2 to 6 are treated with a *strong nonlinear* procedure taking into account the physical data outside the domain *and* the physical state of the computational domain lying near the boundary. In particular, an "inflow" boundary is not incompatible with an "outgoing flux" (i.e. $\phi_1 \equiv \rho u$ negative) for very particular states of the evolution as we will see in the next section.

IV - NUMERICAL EXPERIMENTS WITH THE EXPLICIT FIRST ORDER OSHER SCHEME

In this section we demonstrate the capability of our boundary conditions for several classical monodimensional test cases : shock tube and nozzles. We have implemented a first order method (in space and time) but we choose non-standard initial conditions. We first describe the treatment of the source term for quasi-monodimensional nozzles, then we review the SOD shock tube [42] and test problems on the Laval nozzle presented by GRIFFIN-ANDERSON [22] and the diverging nozzle of SHUBIN-STEPHENS-GLAZ [40].

1 - NUMERICAL SCHEME INCLUDING SOURCE TERMS

The quasi-monodimensional evolution of a perfect fluid in a nozzle of section $y = A(x)$ is given by :

$$(4.1) \qquad (AU)_t + (AF(U))_x - A_x H(U) = 0$$

with conservative variables U and physical flux $F(U)$ given in (2.22)-(2.24) and a source term H such that

$$(4.2) \qquad {}^tH = (0,p,0) \quad .$$

We discretize the interval $[0,1]$ by N cells (i.e. $\Delta x = \frac{1}{N}$). We denote the mean value of U (resp. A,H) on the j° cell $]x_{j-\frac{1}{2}}, x_{j+\frac{1}{2}}[$, with

$$(4.3) \qquad x_{j-\frac{1}{2}} \equiv (j-1)\,\Delta x \quad , \quad j = 1,\ldots,N$$

by U_j (resp. A_j, H_j), and the value of F (resp. A) at the point $x_{j+\frac{1}{2}}$ between cells j and $(j+1)$ by $F_{j+\frac{1}{2}}$ (resp. $A_{j+\frac{1}{2}}$). Integrating the equation (4.1) in space over each cell, we get the semi-discrete version of the scheme :

$$(4.4)\qquad \left\{ \begin{aligned} & A_j \frac{dU_j}{dt} + \frac{1}{\Delta x}\left[A_{j+\frac{1}{2}} F_{j+\frac{1}{2}} - A_{j-\frac{1}{2}} F_{j-\frac{1}{2}}\right] + \\ & \qquad - \frac{1}{\Delta x}\left(A_{j+\frac{1}{2}} - A_{j-\frac{1}{2}}\right) H_j = 0 \quad , \qquad j = 1,\ldots,N \end{aligned} \right.$$

The flux $F_{j+\frac{1}{2}}$ is computed thanks to the Osher numerical flux $\phi(U_j, U_{j+1})$ (formula (2.34)) on each internal interface $(j = 1,\ldots,N-1)$ and thanks to the study done in Section III (formulae (3.1), (3.4), (3.7), (3.17), (3.19)) at the boundary $(j = 0$ or $N)$. The source term H_j is finally given by :

$$(4.5)\qquad H_j = H(U_j) \quad .$$

The explicit numerical scheme is obtained when approaching the system (4.4) of ordinary differential equations by a forward Euler scheme in time. The local time step Δt^n was chosen to satisfy a Courant-Friedrichs-Lewy condition :

$$(4.6)\qquad \frac{\Delta t^n a^n}{\Delta x} = 0.9$$

with a^n equal to the absolute value of the greatest velocity wave involved in the resolution of the $(N+1)$ Riemann problems at the interfaces.

2 - STUDY OF THE SOD SHOCK TUBE

In his classical review [42], SOD compared several numerical schemes for the particular initial conditions :

$$(4.7) \qquad \begin{cases} \rho_L = 1 & u_L = 0 & p_L = 1 \\ \rho_R = 0.125 & u_R = 0 & p_R = 0.1 \end{cases}$$

and plotted results obtained with $N = 100$ cells at time $T = 0.142$ (the 3-shock wave is located at $x = 0.75$). We consider there the steady-state associated to this evolution problem, obtained on the complete $[0,1]$ interval for time $\geqslant 7.112$ and equal to the first intermediate state in the resolution of the Riemann problem (Figure 4.1). During this evolution the 1-rarefaction (resp. 2-contact and 3-shock) is going outside the computational domain to the left ($x = 0$) (resp. the right, $x = 1$). At the boundaries, we take the condition of "state at infinity" (section III-2) naturally associated with that problem.

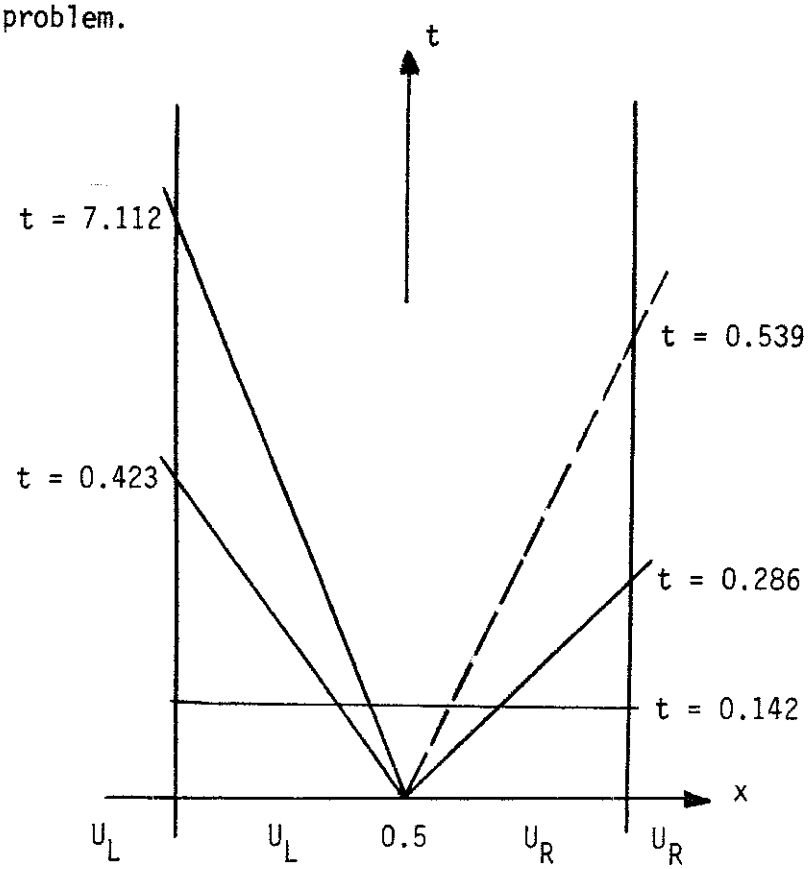

Figure 4.1 The Sod shock tube for time tending to infinity.

The Figure 4.2 (resp. 4.3) shows the computed evolution of velocity (resp. density) in the first (resp. last) cell of the tube after a run of 2500 (resp. 200) time steps. The dotted line is the exact solution. We insist on the fact that the *time evolution* of velocity and density are plotted on Figures 4.2-4.3 which is rather unusual [42]. The interest of these figures lies on the non-reflecting evolution of waves across the boundary rather than on the (poor) accuracy of the results (due to the use of a first-order scheme).

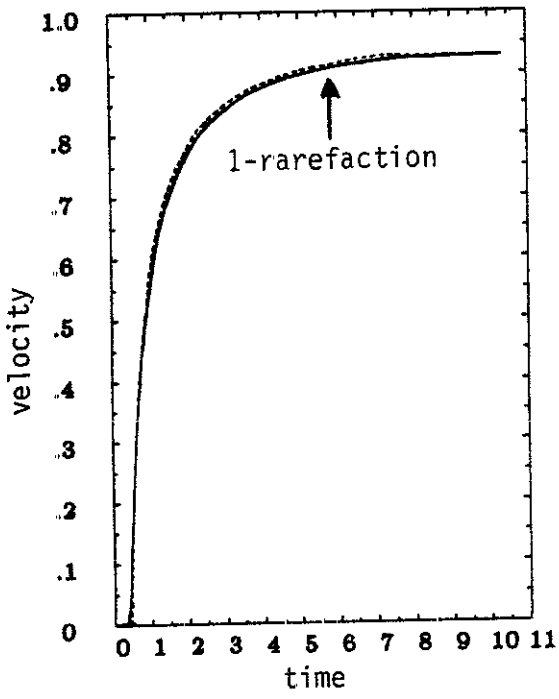

Figure 4.2 Evolution of velocity at x = 0 (dotted line : exact solution). Sod shock tube, N = 100

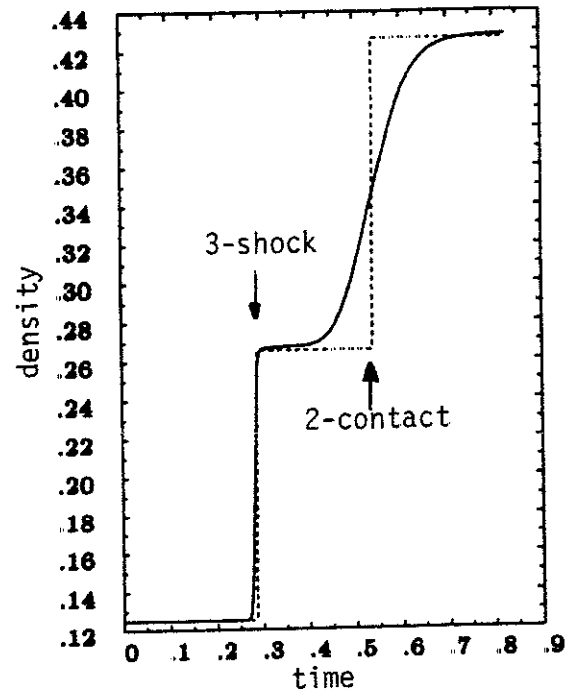

Figure 4.3 Evolution of density at x = 1 (dotted line : exact solution). Sod shock tube, N = 100

3 - STUDY OF A LAVAL NOZZLE

A family of converging-diverging nozzles was introduced by GRIFFIN-ANDERSON [22] and used for testing numerical methods by other authors (e.g. YEE-BEAM-WARMING [50], CASIER-DECONINCK-HIRSCH [7]). We have chosen the section $A(x)$ defined by (Figure 4.4) :

$$A(x) = \begin{cases} 1 + 1.5(1-2x)^2 & 0 \leq x \leq 0.5 \\ 1 + 0.5(1-2x)^2 & 0.5 \leq x \leq 1 \end{cases} \tag{4.8}$$

and two test cases associated with the following boundary conditions :

Test 1 : subsonic inflow and outflow (with a shock wave)

Test 2 : subsonic inflow and supersonic outflow.

In both cases the input data are given as in section III-5, i.e.

$$H = 3 \quad , \quad \Sigma = 1 \qquad (x = 0) \tag{4.9}$$

and for test case 1, the out (static) pressure is :

$$P = 0.4 \quad . \tag{4.10}$$

We now focus on the initial condition for such computations. For tests similar to test 1, a majority of authors (e.g. YEE-BEAM-WARMING [50], CASIER-DECONINCK-HIRSCH [7]) take a linear interpolation between the exact boundary values. The situation is identical for test 2 [7]. We have performed computations with success in these two cases using that type of initial conditions although they are not natural (in test 1 for example the exact knowledge of the right boundary value is nearly equivalent to the entire exact solution). Following CHAKRAVARTHY [8] we think that a natural initial condition for both tests is the stagnation state (with null velocity) associated with (4.9), along the whole channel, i.e.

$$\rho_i \equiv 0.680 \quad , \quad u_i \equiv 0 \quad , \quad p_i \equiv 0.583 \tag{4.11}$$

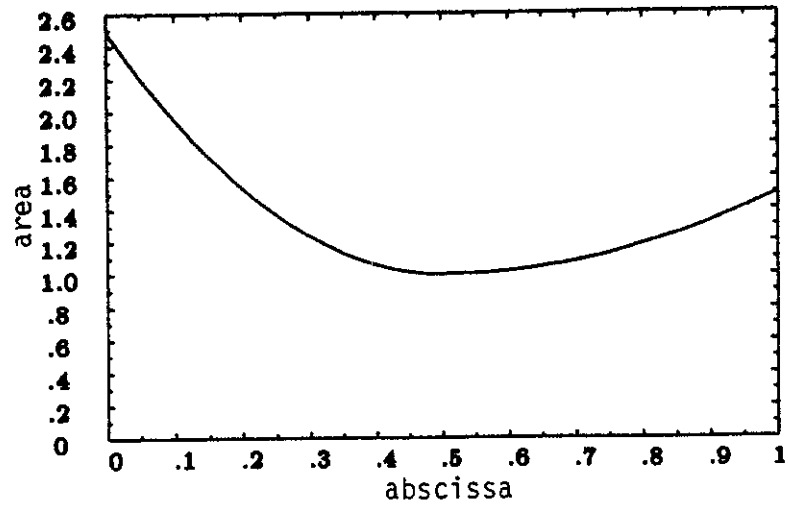

Figure 4.4 Area variation of the Laval nozzle [22]

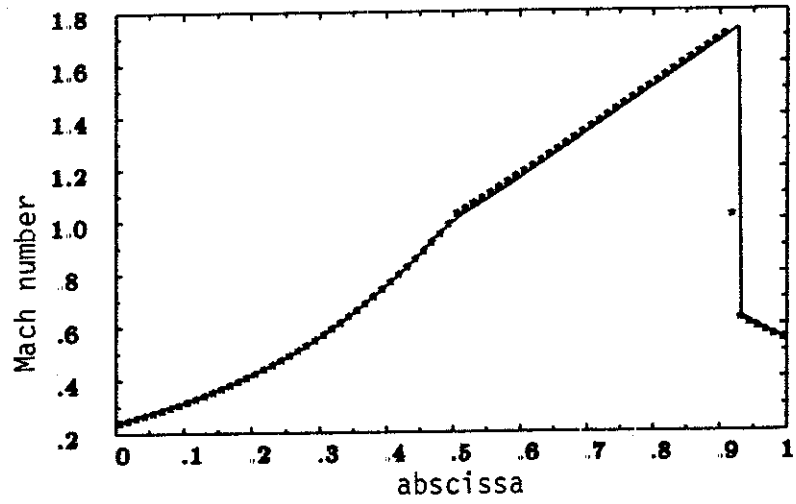

Figure 4.5 Mach number at convergence, test 1 (subsonic inflow and outflow), stars : computed, line : exact. Laval nozzle, N = 80.

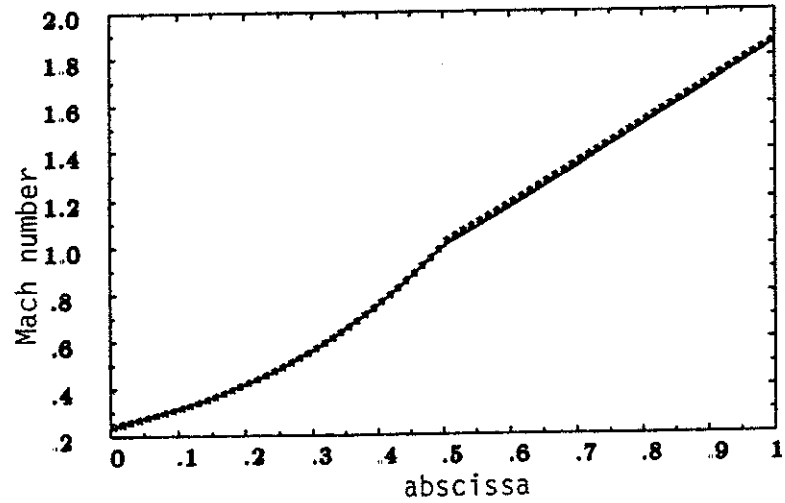

Figure 4.6 Mach number at convergence, test 2 (subsonic inflow and supersonic outflow), stars : computed, line : exact. Laval nozzle, N = 80

We have taken (4.11) as the initial condition for both test-cases, refining the mesh (N = 20,40,80). The machine accuracy (32 bits computer) was obtained after 1600 time steps for test 1 and 1000 for test 2 (with N = 80). Figures 4.5 and 4.6 show the converged distributions of Mach number. The residual of momentum for test 1 is displayed on Figure 4.7.

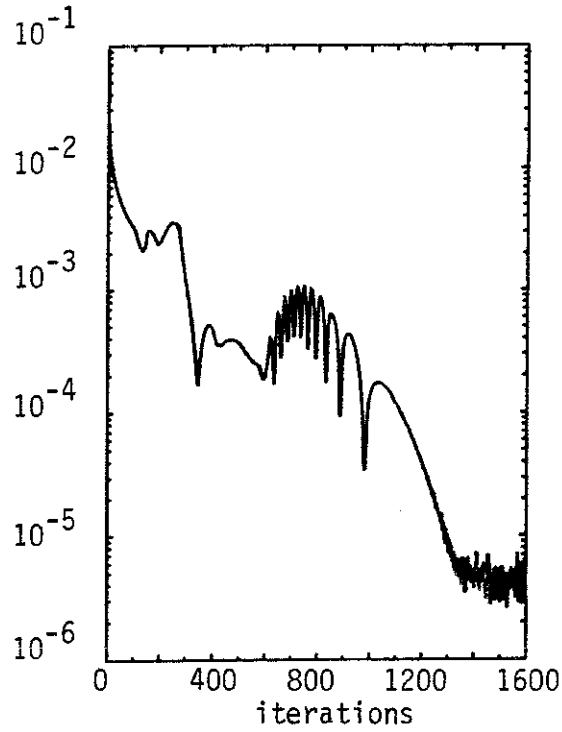

Figure 4.7 Residual of momentum, test 1. Laval nozzle, N = 80.

Typical evolution of velocity for both test cases are presented on Figures 4.8 and 4.9 and similar curves have been obtained for density and pressure.

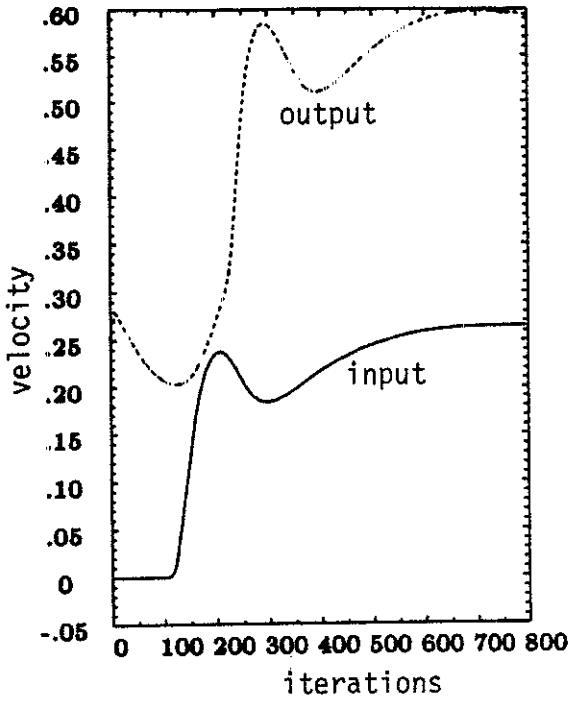

Figure 4.8

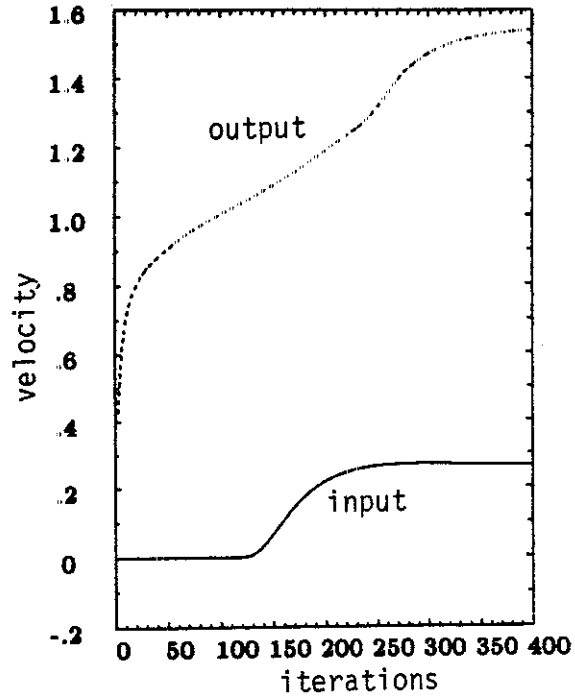

Figure 4.9

Evolution of velocity at $x = 0$ (straight line) and at $x = 1$ (dotted line), for test 1 (subsonic inflow and outflow, Figure 4.8) and test 2 (subsonic inflow and supersonic outflow, Figure 4.9). Laval nozzle, $N = 80$.

4 - TEST CASES INVOLVING A DIVERGING NOZZLE

The diverging channel proposed by SHUBIN-STEPHENS-GLAZ [40] has a section $A(x)$ displayed on Figure 4.10 and satisfying

$$A(x) = 1.398 + 0.347 \tanh(8x-4) \quad , \quad 0 \leqslant x \leqslant 1 \quad . \tag{4.12}$$

The left boundary condition is a supersonic inflow :

$$\rho_L = 0.502 \quad , \quad u_L = 1.299 \quad , \quad p_L = 0.381 \quad . \tag{4.13}$$

As in the above section, test 1 is concerned with a subsonic outflow of pressure P :

$$P = 0.707 \tag{4.14}$$

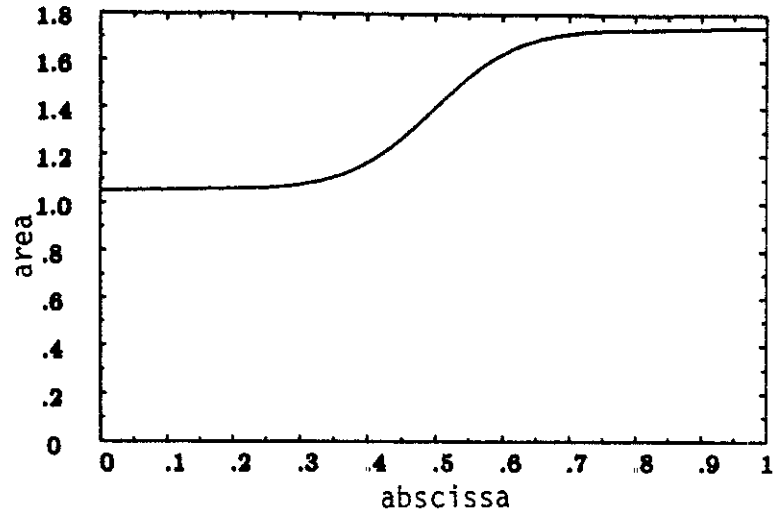

Figure 4.10 Area variation of the diverging nozzle [40].

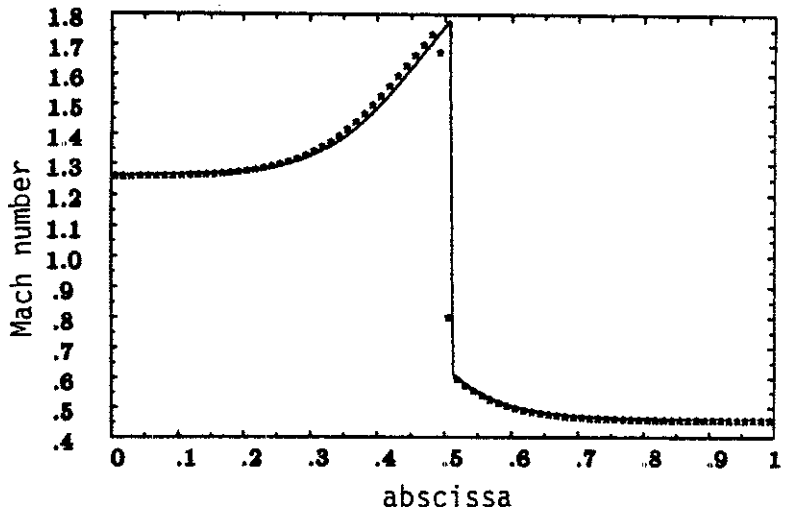

Figure 4.11 Mach number at convergence (stars : computed, line : exact). Test 1 (supersonic inflow, subsonic outflow). Diverging nozzle, N = 80.

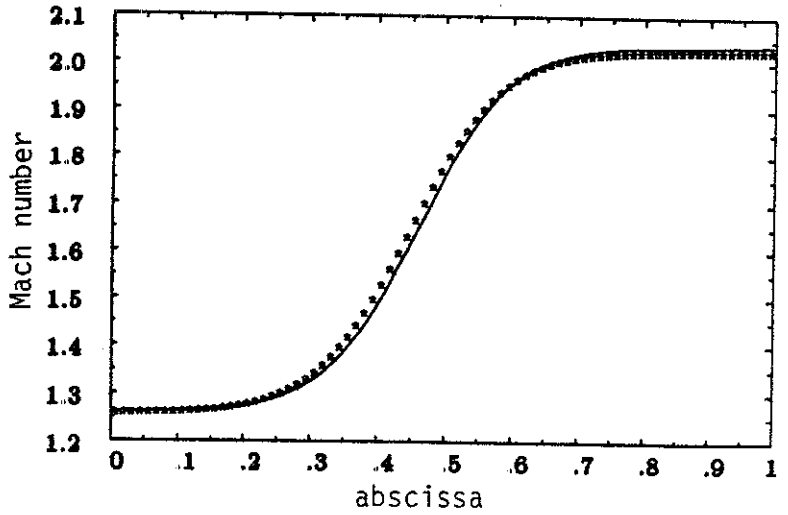

Figure 4.12 Mach number at convergence (stars : computed, line : exact). Test 2 (supersonic inflow and outflow). Diverging nozzle, N = 80.

inducing a shock wave located at $x = 0.5$. Test 2 is related to a supersonic outflow. We have chosen, as above, stagnation initial conditions associated with (4.13), i.e.

(4.15) $\qquad \rho_i \equiv 1 \quad , \quad u_i \equiv 0 \quad , \quad p_i \equiv 1$

and three meshes of $N = 20,40,80$ cells. On the most refined mesh, machine accuracy was obtained after 1600 iterations. The converged isomach curves are plotted on Figures 4.11 and 4.12. The evolution of velocity for both test cases is given on Figures 4.13 and 4.14. No particular problem of convergence was given by these initial-boundary value problems with our treatment of the boundary conditions.

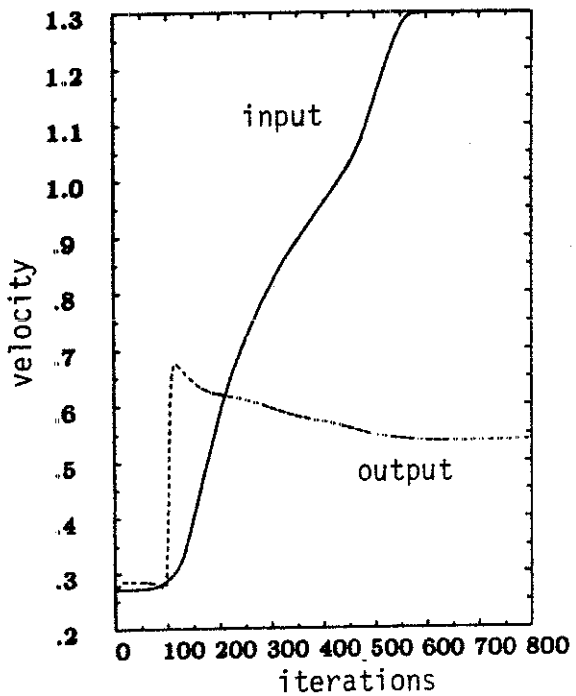

Figure 4.13

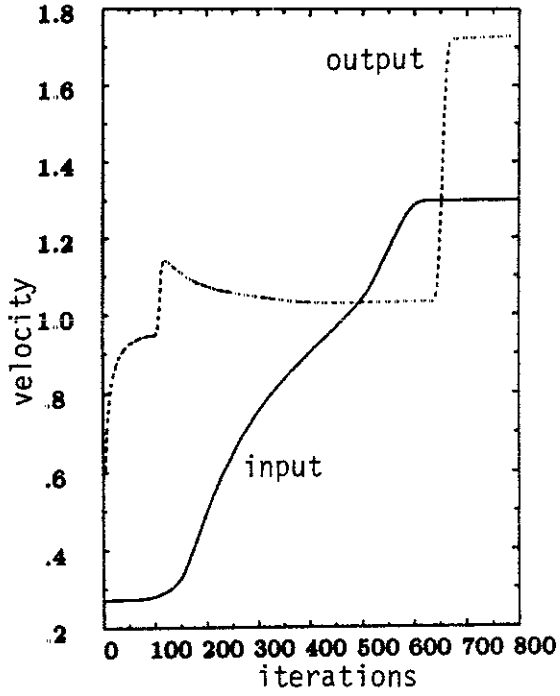

Figure 4.14

Evolution of velocity at $x = 0$ (straight line) and at $x = 1$ (dotted line). Test 1 (supersonic inflow and subsonic outflow, Figure 4.13) and Test 2 (supersonic inflow and outflow, Figure 4.14). Diverging nozzle, $N = 80$.

To demonstrate the robustness of our method we have computed test case 2 (supersonic flow) on a $N = 20$ mesh points with the *same static initial condition* (4.15) but changing the treatment of boundary conditions. In a first experiment (test 2.a) we have taken the numerical flux at supersonic inflow following the classical treatment : the numerical flux is given by the (left) boundary data rather than by the Riemann problem (3.1), i.e. :

$$\phi(x = 0) = f(U_L) \quad . \tag{4.16}$$

On the right, we kept the treatment given by formula (3.19). In a second investigation (test 2.b), we have kept the treatment (3.1) on the inflow and changed the outflow, replacing (3.19) by the usual linearized condition for supersonic outflow :

$$\phi(x = 1) = f(U_N) \quad . \tag{4.17}$$

Results are very interesting and surprising. In test 2.a, the right supersonic solution is obtained, after a very long transient evolution of 2400 time steps, that we can compare with the treatment using both (3.1) and (3.19), where numerical convergence arises after 400 time steps (Figure 4.15). With the second choice of boundary conditions (test 2.b), the convergence is very quick (200 iterations) but we obtain a subsonic (!) solution without any simple relation with data (4.13) and stable under mesh refinement. The exact and computed Mach numbers are compared on Figure 4.16. Moreover, with the same pair of boundary conditions (3.1)-(4.17) the initial conditions (4.11) give another subsonic solution. These unrealistic results are a consequence of the "bad" choice (4.15) of initial conditions. Results become correct once more when we start the computation with a supersonic state e.g. (4.13).

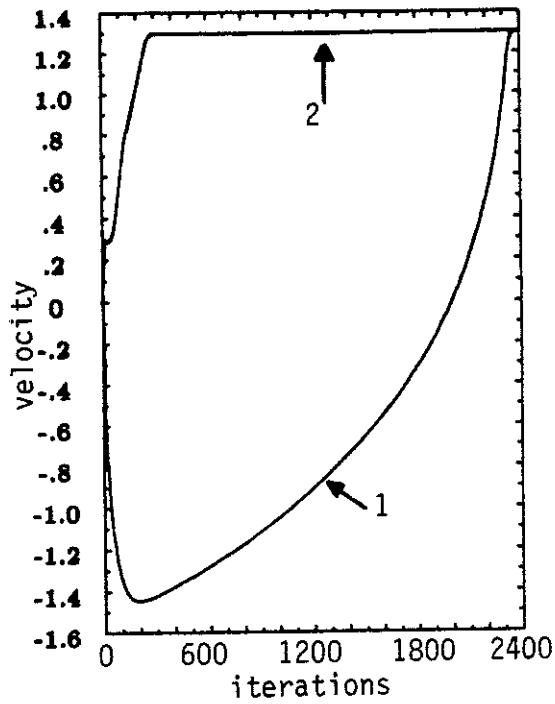

Figure 4.15 Evolution of velocity at $x = 0$ with classical boundary condition (4.16) [curve 1], and new boundary condition (3.1) on inflow (test 2.a). Diverging nozzle, $N = 20$.

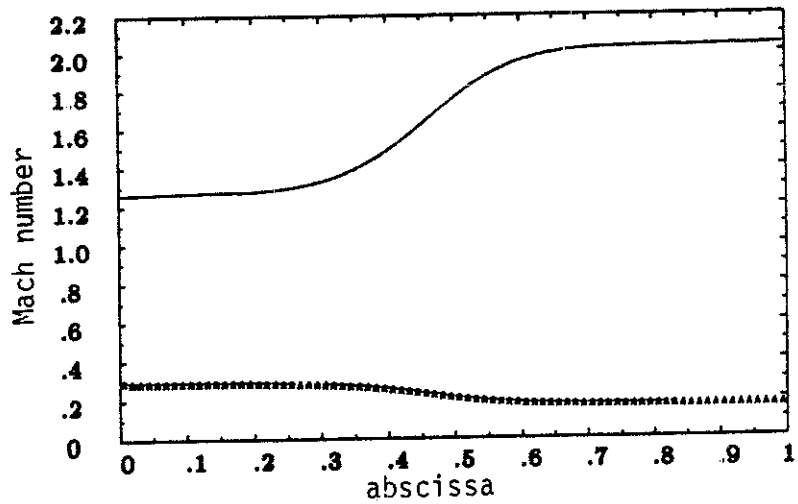

Figure 4.16 Converged Mach number (stars) and exact solution (straight line) for test 2.b (inflow boundary condition (3.1), classical outflow 4.17). Diverging nozzle, $N = 80$.

Nevertheless, we have tried to compute the same test 2 with the treatment (3.1)(3.19) of supersonic in/out flow, but with an inappropriate initial condition, reversing the speed u_L :

(4.18) $\rho_i \equiv 0.502$, $u_i \equiv -1.299$, $p_i \equiv 0.381$

To our surprise, the correct converged state (Figure 4.12) is obtained after a relatively quick evolution (1600 iterations). Velocity and pressure are plotted on Figures 4.17 and 4.18.

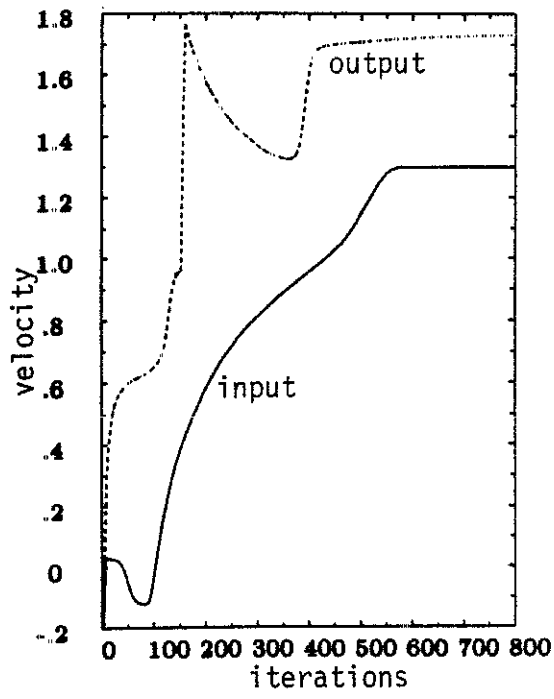

Figure 4.17

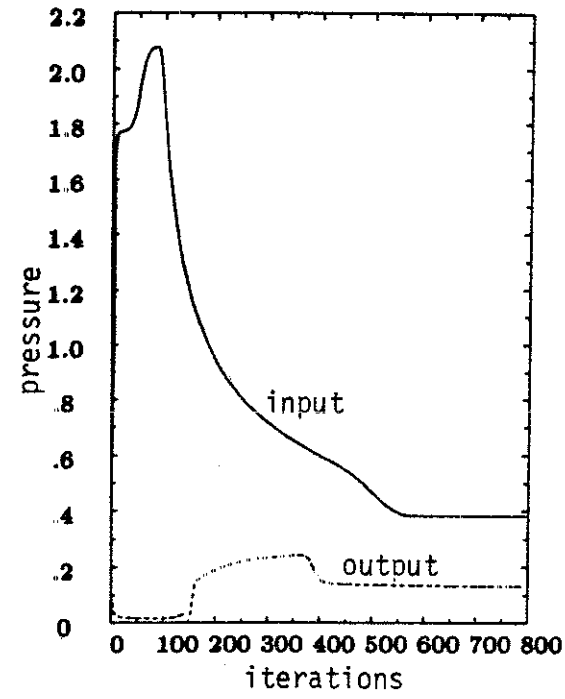

Figure 4.18

Evolution of velocity and static pressure at $x = 0$ (staight line) and at $x = 1$ (dotted line). Test 2 (supersonic flow), initialization by (4.18). Diverging nozzle, $N = 80$.

5 - CONCLUSION

We have proved that the numerical boundary conditions proposed in Section III are robust. The transient evolution converges quickly to the desired steady-state even when initial conditions are a priori far from it. The exact nonlinear interaction between transient waves and stationary waves in a 1D nozzle is analysed by GLAZ-LIU [17] and the behaviour in the vicinity of the steady-state is studied in ENGQUIST-GUSTAFSSON [13] and including references.

V - LINEARIZED IMPLICIT VERSION OF THE SCHEME

We first study the derivability of the flux functions associated with the internal scheme (the Osher scheme in Section II) and the boundaries (Section III). Then explicit formulae allowing an exact computation of the above gradients are given. Empirically CFL numbers related to the test cases of Section IV show the advantage of using a simple linearized implicit scheme.

1 - DERIVABILITY OF THE OSHER SCHEME

The general expression of the Osher flux function given in (2.11) is not a priori clearly derivable due to the step functions ε defined in (2.9)-(2.10). This is also the case for the boundary conditions (3.1), (3.4), (3.7), (3.17), (3.19) related to the Euler equations. We now prove that it is easy to derive (2.11). The results are similar for each particular boundary condition.

PROPOSITION 5.1

Under the hypotheses reviewed in Section I (fields either genuinely nonlinear or linearly degenerated, existence of k*-curves* $\mathscr{W}_k$*), the Oher flux function* (2.11) *associated with the resolution of the multivalued Riemann problem* R(u,v) *is continuously derivable relatively to the pair* (u,v) *and we have :*

$$d\phi(u,v) = \sum_{k=0}^{n} \varepsilon_k f'(u_k) \cdot \left(\frac{\partial u_k}{\partial u} du + \frac{\partial u_k}{\partial v} dv \right) + \sum_{k=1}^{n} \varepsilon'_k f'(u'_k) \cdot \left(\frac{\partial u'_k}{\partial u} du + \frac{\partial u'_k}{\partial v} dv \right) . \tag{5.1}$$

PROOF OF PROPOSITION 5.1

The derivability of $u_k(u,v)$ and $u'_k(u,v)$ is classical because they are solutions of a differential equation and u,v are the associated initial conditions. We simply focus on the discontinuous functions ε,ε' involved in the computation of ϕ. In the proof of Theorem 2.1, $\phi(u,v)$ is given by the formula (2.17), i.e.

$$\phi(u,v) = f(v) - \sum_{k=1}^{n} \chi(\lambda_k(u_k))(f(u_k) - f(u'_k)) + - \sum_{k=0}^{n-1} \chi(\lambda_{k+1}(u_k))(f(u'_{k+1}) - f(u_k)) \quad . \tag{5.2}$$

where χ is the Heaviside function. Deriving (5.2) in the sense of distributions, the first part obtained by deriving only the f-terms clearly gives (5.1). The second part is a sum of f, times the derivatives of Heaviside functions. But if $\lambda_k(u_k)$ (resp. $\lambda_{k+1}(u_k)$) is null, then $u'_k = u_k$ (resp. $u'_{k+1} = u_k$) and the coefficient of the Dirac function vanishes. Thus (5.1) is established in the case of all genuinely nonlinear fields. We then conclude the proof with the same arguments as in Theorem 2.1. ∎

2 - COMPUTATION OF THE FLUX GRADIENTS

We now specify the formulae associated with the interior scheme and the boundary scheme for the particular case of the Euler equations.

The variables W (2.26) are naturally associated with the computation of intermediate states U_1', U_1, U_2, U_3' that we denote by $\tilde{U}$. Then the derivative of $F(\tilde{U})$ with respect to (U_L, U_R) is given by the chain rule :

$$(5.3) \qquad dF(\tilde{U}) = \sum_{J=L,R} \frac{\partial F}{\partial W}(\tilde{U}) \cdot \frac{\partial W}{\partial W_J}(\tilde{W}) \cdot \frac{\partial W_J}{\partial U_J}(U_J)\, dU_J$$

with $W_J = W(U_J)$ and $\tilde{W} = W(\tilde{U})$. From (2.24)-(2.28), we deduce

$$(5.4) \qquad F(W) = \begin{pmatrix} \rho u & = \alpha\, c^{\frac{2}{\gamma-1}}\, \sigma^{-\frac{2\gamma}{\gamma-1}}\, u \\ \rho u^2 + p & = \alpha\, c^{\frac{2}{\gamma-1}}\, \sigma^{-\frac{2\gamma}{\gamma-1}}\, u^2 + \beta\, c^{\frac{2\gamma}{\gamma-1}}\, \sigma^{-\frac{2\gamma}{\gamma-1}} \\ \rho u E + p u & = \frac{\alpha}{2}\, c^{\frac{2}{\gamma-1}}\, \sigma^{-\frac{2\gamma}{\gamma-1}}\, u^3 + \frac{\gamma}{\gamma-1}\, \beta\, c^{\frac{2\gamma}{\gamma-1}}\, \sigma^{-\frac{2\gamma}{\gamma-1}}\, u \end{pmatrix}$$

with $\alpha = \gamma^{-1/\gamma-1}$ and $\beta = \alpha^{\gamma}$,

$$(5.5) \qquad \frac{\partial F}{\partial W} = \begin{pmatrix} \frac{2}{\gamma-1}\frac{\rho u}{c} & ; \quad \rho & ; \quad -\frac{2\gamma}{\gamma-1}\frac{\rho u}{\sigma} \\ \frac{2}{\gamma-1}\frac{\rho u^2}{c} + \frac{2\gamma}{\gamma-1}\frac{p}{c} & ; \quad 2\rho u & ; \quad -\frac{2\gamma}{\gamma-1}\frac{\rho u^2}{\sigma} - \frac{2\gamma}{\gamma-1}\frac{p}{\sigma} \\ \frac{\rho u^3}{(\gamma-1)c} + \frac{2\gamma}{\gamma-1}\frac{\gamma}{\gamma-1}\frac{pu}{c} & ; \frac{3}{2}\rho u^2 + \frac{\gamma p}{\gamma-1} & ; -\frac{\gamma}{\gamma-1}\frac{\rho u^3}{\sigma} - \frac{2\gamma}{\gamma-1}\frac{\gamma}{\gamma-1}\frac{pu}{\sigma} \end{pmatrix}$$

and similarly :

$$(5.6) \qquad \frac{\partial W}{\partial U} = \begin{pmatrix} -\frac{1}{2}\frac{c}{\rho} + \frac{\gamma-1}{4}\frac{cu^2}{p} & -\frac{\gamma-1}{2}\frac{cu}{p} & \frac{\gamma-1}{2}\frac{c}{p} \\ -\frac{u}{\rho} & \frac{1}{\rho} & 0 \\ -\frac{\sigma}{2\rho} + \frac{\gamma-1}{4\gamma}\frac{\sigma u^2}{p} & -\frac{\gamma-1}{2\gamma}\frac{\sigma u}{p} & \frac{\gamma-1}{2\gamma}\frac{\sigma}{p} \end{pmatrix}$$

We only have to specify the computation of factors $\frac{\partial W}{\partial W_J}(\tilde{W})$ in (5.3), for $\tilde{U} = U_1', U_2, U_3, U_3'$ and $J = L, R$ to be able to compute (5.1). This is a consequence of elementary algebraic derivations of (2.29)-(2.32) and we get :

$$(5.7)\qquad \frac{\partial W_1'}{\partial W_L}(U_1') = \begin{pmatrix} \frac{2}{\gamma+1} & \frac{\gamma-1}{\gamma+1} & 0 \\ \frac{2}{\gamma+1} & \frac{\gamma-1}{\gamma+1} & 0 \\ 0 & 0 & 1 \end{pmatrix}, \qquad \frac{\partial W}{\partial W_R}(U_1') = 0$$

$$(5.8)\qquad \frac{\partial W_1}{\partial W_L}(U_1) = \begin{pmatrix} \frac{1}{1+\sigma_R/\sigma_L} & \frac{\gamma-1}{2(1+\sigma_R/\sigma_L)} & \frac{c_1}{\sigma_L(1+\sigma_L/\sigma_R)} \\ \frac{2}{(\gamma-1)(1+\sigma_L/\sigma_R)} & \frac{1}{1+\sigma_L/\sigma_R} & \frac{-2c_1}{(\gamma-1)\sigma_L(1+\sigma_L/\sigma_R)} \\ 0 & 0 & 1 \end{pmatrix}$$

$$(5.9)\qquad \frac{\partial W_1}{\partial W_R}(U_1) = \begin{pmatrix} \frac{1}{1+\sigma_R/\sigma_L} & \frac{-(\gamma-1)}{2(1+\sigma_R/\sigma_L)} & \frac{-c_1}{\sigma_L+\sigma_R} \\ \frac{-2}{(\gamma-1)(1+\sigma_R/\sigma_L)} & \frac{1}{1+\sigma_R/\sigma_L} & \frac{2c_1}{(\gamma-1)(\sigma_L+\sigma_R)} \\ 0 & 0 & 0 \end{pmatrix}$$

$$(5.10)\qquad \frac{\partial W_2}{\partial W_L}(U_2) = \begin{pmatrix} \frac{1}{1+\sigma_L/\sigma_R} & \frac{\gamma-1}{2(1+\sigma_L/\sigma_R)} & \frac{-c_2}{\sigma_L+\sigma_R} \\ \frac{2}{(\gamma-1)(1+\sigma_L/\sigma_R)} & \frac{1}{1+\sigma_L/\sigma_R} & \frac{-2c_2}{(\gamma-1)(\sigma_L+\sigma_R)} \\ 0 & 0 & 0 \end{pmatrix}$$

$$(5.11)\qquad \frac{\partial W_2}{\partial W_R}(U_2) = \begin{pmatrix} \frac{1}{1+\sigma_L/\sigma_R} & \frac{-(\gamma-1)}{2(1+\sigma_L/\sigma_R)} & \frac{c_2}{\sigma_R(1+\sigma_R/\sigma_L)} \\ \frac{-2}{(\gamma-1)(1+\sigma_R/\sigma_L)} & \frac{1}{1+\sigma_R/\sigma_L} & \frac{2c_2}{(\gamma-1)\sigma_R(1+\sigma_R/\sigma_L)} \\ 0 & 0 & 1 \end{pmatrix}$$

$$(5.12)\qquad \frac{\partial W_3'}{\partial W_L}(U_3') = 0\ ,\ \frac{\partial W_3'}{\partial W_R}(U_3') = \begin{pmatrix} -\frac{2}{\gamma+1} & \frac{\gamma-1}{\gamma+1} & 0 \\ \frac{2}{\gamma+1} & \frac{-(\gamma-1)}{\gamma+1} & 0 \\ 0 & 0 & 1 \end{pmatrix}$$

• We now consider the derivation of the boundary flux functions described in Section III. In the particular cases of a given state at infinity, wall reflection and supersonic inflow, a formula similar to (5.1) is easily obtained by the previous considerations. In the particular case (3.7) of subsonic outflow (resp. (3.17), subsonic inflow) the intermediate state U_1 (and U_2 for the outflow) are computed thanks to formulae (3.6) (resp. (3.15)-(3.16)). We now give the new formulae for the $\partial W/\partial W'$s.

* *Subsonic outflow* (P is given)

The state U_1 is computed thanks to (3.6). Then we have :

$$(5.13)\qquad \frac{\partial W_1^P}{\partial W_L}(U_1) = \begin{pmatrix} 0 & 0 & \frac{c_1}{\sigma_L} \\ \frac{2}{\gamma-1} & 1 & -\frac{2}{\gamma-1}\frac{c_1}{\sigma_L} \\ 0 & 0 & 1 \end{pmatrix}$$

* *Subsonic inflow* (H and Σ are given)

The intermediate states U_1 and U_2 are given in (3.15) and (3.16). Setting

$$(5.14)\qquad \delta = \sqrt{2\left(1+\frac{\gamma-1}{2}\left(\frac{\Sigma}{\sigma_R}\right)^2\right)H - \frac{\gamma-1}{2}\left(\frac{\Sigma}{\sigma_R}\right)^2\left(u_R - \frac{2}{\gamma-1}c_R\right)^2}$$

we have

$$(5.15)\qquad \frac{\partial W_1^{HS}}{\partial W_R}(U_1) = \begin{pmatrix} \frac{\Sigma}{\sigma_R}\frac{u_1}{\delta} & -\frac{\gamma-1}{2}\frac{\Sigma}{\sigma_R}\frac{u_1}{\delta} & -\frac{c_1}{\sigma_R}\frac{u_1}{\delta} \\ -\frac{2}{\gamma-1}\frac{\Sigma}{\sigma_R}\frac{c_1}{\delta} & \frac{\Sigma}{\sigma_R}\frac{c_1}{\delta} & \frac{2}{\gamma-1}\frac{c_1^2}{\delta\sigma_R} \\ 0 & 0 & 0 \end{pmatrix}$$

$$(5.16)\qquad \frac{\partial W_2^{HS}}{\partial W_R}(U_2) = \begin{pmatrix} \frac{u_2}{\delta} & -\frac{\gamma-1}{2}\frac{u_2}{\delta} & \frac{c_2}{\sigma_R}\left(1-\frac{u_2}{\delta}\right) \\ -\frac{2}{\gamma-1}\left(\frac{\Sigma}{\sigma_R}\right)^2\frac{c_2}{\delta} & \left(\frac{\Sigma}{\sigma_R}\right)^2\frac{c_2}{\delta} & \frac{2}{\gamma-1}\left(\frac{\Sigma}{\sigma_R}\right)^2\frac{c_2^2}{\delta\sigma_R} \\ 0 & 0 & 1 \end{pmatrix}$$

The formulae given above allow an *exact* derivation of both the numerical Osher flux (internal interfaces) *and* the boundary fluxes. As noticed by RAI-CHAKRAVARTHY [37], these computations are expensive but we do not consider them as a "tedious procedure" with our presentation. All the 3×3 matrices computations have been implemented in a vectorizable computer program.

3 - NUMERICAL TESTS OF THE LINEARIZED IMPLICIT SCHEME

From the previous study, an implicit version of the numerical scheme used in Section IV can be derived, as proposed by RAI-CHAKRAVARTHY [37]. Starting from the system of ODE (4.4), i.e.

$$(5.17)\qquad \frac{dU_j}{dt} + G_j(\{U\}) = 0 \qquad , \qquad j = 1,\ldots,N$$

with

$$(5.18)\qquad \left\{ G_j(\{U\}) = \frac{A_{j+\frac{1}{2}}}{\Delta x\, A_j}\left[\phi(U_j,U_{j+1}) - H(U_j)\right] + \right.$$
$$\left. - \frac{A_{j-\frac{1}{2}}}{\Delta x\, A_j}\left[\phi(U_{j-1},U_j) - H(U_j)\right] \quad , \quad j = 2,\ldots,N-1 \right.$$

The backward Euler scheme

$$(5.19)\qquad \frac{1}{\Delta t}\,(U_j^{n+1} - U_j^n) + G_j(\{U^{n+1}\}) = 0$$

is linearized around $\{U^n\}$. Then we obtain the linearized implicit scheme :

$$(5.20)\qquad \frac{1}{\Delta t}\,(U_j^{n+1} - U_j^n) + \frac{\partial G_j}{\partial U}\cdot(U^{n+1} - U^n) = -\,G_j(\{U^n\})$$

The matrix $\frac{\partial G_j}{\partial U}$ is entirely known from the computation of $d\phi_{j+\frac{1}{2}}$ and dH_j. The term $d\phi_{j+\frac{1}{2}}$ has been treated in previous section. Thanks to (4.2), the gradient of pressure

$$(5.21)\qquad dp = (\gamma-1)\left(\frac{u^2}{2}, -u, 1\right) dU$$

completely defines dH_j.

We have tested the scheme (5.20) on two problems considered in Section IV : The Sod shock tube and the diverging nozzle for both tests 1 and 2. We used mesh refinements, a variation of the initial conditions and for each test case, the computations have been carried out down to machine accuracy. Accurate results are summarized in Table 5.1. In each case, we have determined experimentally a maximal CFL number (see condition (4.6)). The Sod shock tube is a transient problem, containing moving nonlinear waves. The CFL = 7 observed in this case is worse than in

other computations converging to a steady state. Nevertheless our CFL numbers can be compared to the results previously given by RAI-CHAKRAVARTHY [37] with the same basic scheme but with an other treatment of the boundary conditions [8].

Test case	Maximal CFL number (experimental)
• Sod shock tube [42], N = 20,40,100	7
• Diverging nozzle [40], N = 20,40,80 with supersonic inflow (boundary condition (3.1))	
1) subsonic outflow (4.14)	
* Initial condition : stagnation (4.15)	10
* Initial condition : state (4.13)	20
2) supersonic outflow	
* Initial condition : stagnation (4.15)	10
* Initial condition : linear interpolation of variables (ρ,u,p) between the limiting states of the exact solution.	50

Table 5.1 Numerical tests of the linearized implicit scheme

CONCLUSION

In this paper we have extended a proposal of VAN LEER [45] and OSHER [36]. We have also given a new presentation of the Osher scheme. This scheme can be viewed as a Godunov-type scheme involving a multivalued solution of a Riemann problem as well as a splitting scheme. The previous theoretical vision of the boundary conditions for the Euler equations proposed in [10] by DUBOIS-LE FLOCH has lead to a numerical treatment of the flux at the boundary. The latter is computed thanks to partial Riemann problems (depending on the given physical quantity) evaluated by multivalued solutions. The derivation of a linearized implicit scheme following this approach is straightforward. Numerical experiments have proved the robustness of both explicit and implicit schemes with respect to the dependance on initial condition and/or time step.

This work can be extended by both numerical and theoretical studies. On the one hand, second order two-dimensional and nonlinear implicit versions of the scheme are under development. On the other hand, our boundary conditions appear as non-reflecting. The link with the previous work of HEDSTRÖM [27] and other classical studies on absorbing conditions (e.g. [14,3,24] and including references) is still to be done.

ACKNOWLEDGMENTS

I thank Yann Brenier for our helpfull discussions about this work.

REFERENCES

[1] AUDOUNET J., *Solutions discontinues paramétriques des systèmes de lois de conservation et des problèmes aux limites associés*, Seminar, Toulouse III univ., 1983-84.

[2] BARDOS C., LEROUX A.Y., NEDELEC J.C., *First order Quasilinear Equations with Boundary Conditions*, Comm P.D.E. vol 4, n° 9, pp 1017-1034, 1979.

[3] BAYLISS A., TURKEL E., *Outflow Boundary Conditions for Fluid Dynamics*, SIAM J., Sci. Stat. Comput. vol 3, n° 2, pp 250-259, 1982.

[4] BRENIER Y., *Averaged Multivalued Solutions for Scalar Conservation Laws*, SIAM J. Numer Anal, vol 21, n° 6, pp 1013-1037, 1984.

[5] BRENIER Y., *A Time Discretization for Conservation Laws*, in Numerical Methods for the Euler Equations of Fluid Dynamics (Angrand et al, Eds), SIAM, Philadelphia, pp 108-120, 1985.

[6] BRENIER Y., OSHER S., *Approximate Riemann Solvers and Numerical Flux Functions*. SIAM J. Numer Anal, vol 23, n° 2, pp 259-273, 1986.

[7] CASIER F., DECONINCK H., HIRSCH C., *A Class of Bidiagonal Schemes for Solving the Euler Equations*. AIAA J. vol 22, n° 11, pp 1556-1563, 1984.

[8] CHAKRAVARTHY S., *Euler Equations - Implicit Schemes and Boundary Conditions*. AIAA J., vol 1, n° 5, pp 699-706, 1983.

[9] CHAKRAVARTHY S., OSHER S., *Numerical Experiments with the Osher Upwind Scheme for the Euler Equations*. AIAA J., vol 21, n° 9, pp 1241-1248, 1983.

[10] DUBOIS F., LE FLOCH P., *Condition à la limite pour un système de lois de conservation*. C.R. Acad. Sc. Paris, t 304, Serie 1, n° 3, pp 75-78, 1987.

[11] DUBOIS F., LE FLOCH P., *Boundary Conditions for Nonlinear Systems of Conservation Laws*. J. of Diff. Equations, to appear.

[12] DUKOWICZ J., *A General, Non-Iterative Riemann Solver for Godunov's Method*. J of Comp. Phys., vol 61, pp 119-137, 1985.

[13] ENGQUIST B., GUSTAFSSON B., *Steady State Computations for Wave Propagation Problems*. Maths of Comp, vol 49, n° 179, pp 39-64, 1987.

[14] ENGQUIST B., MAJDA A., *Numerical Radiation Boundary Conditions for Unsteady Transonic Flow*. J. of Comp. Phys, vol 40, pp 91-103, 1981.

[15] ENGQUIST B., OSHER S., *Stable and Entropy Satisfying Approximations for Transonic Flow Calculations*. Math of Comp, vol 34, pp 45-75, 1980.

[16] ENGQUIST B., OSHER S., *One-Sided Difference Approximations for Nonlinear Conservation Laws*, Math of Comp, vol 36, pp 321-352, 1981.

[17] GLAZ H., LIU T.P., *The Asymptotic Analysis of Wave Interactions and Numerical Calculations of Transonic Nozzle Flow*. Advances in Appl. Maths, vol 5, pp 111-146, 1984.

[18] GODUNOV S.K., *A Finite Difference Method for the Numerical Computation of Discontinuous Solutions of the Equations of Fluid Dynamics*. Mat. Sb. vol 47, pp 271-290, 1959.

[19] GODUNOV S.K. et coll, *Résolution Numérique des Problèmes Multidimensionnels de la Dynamique des Gaz*. Editions MIR, Moscou, 1979, 1976.

[20] GOLDBERG M., TADMOR E., *Convenient Stability Criteria for Difference Approximations of Hyperbolic Initial-Boundary Value Problems II*. Math. of Comp., vol 48, n° 178, pp 503-520, 1987.

[21] GOODMANN J., *Initial Boundary Value Problems for Hyperbolic Systems of Conservation Laws*. Ph D Thesis, California Univ, 1982.

[22] GRIFFIN M., ANDERSON J.D., *On the Application of Boundary Conditions to Time Dependent Computations for Quasi One-Dimensional Fluid Flows*. Comp. & Fluids, vol 5, pp 127-137, 1977.

[23] GUSTAFSSON B., KREISS H.O., SUNDSTRÖM A., *Stability Theory of Difference Approximations for Mixed Initial Boundary Value Problems*. Math of Comp, vol 26, pp 649-686, 1972.

[24] HALPERN L., SCHATZMAN M., *Artificial Boundary Conditions for Incompressible Viscous Flows*, Internal Report n° 162, Ecole Polytechnique, Centre de Mathématiques Appliquées, Palaiseau, 1987.

[25] HARTEN A., LAX P.D., *A Random Choice Finite Difference Scheme for Hyperbolic Conservation Laws*. SIAM J. Numer Anal, vol 18, n° 2, pp 289-315, 1981.

[26] HARTEN A., LAX P.D., VAN LEER B., *On Upstream Differencing and Godunov-type Schemes for Hyperbolic Conservation Laws*. SIAM Review, vol 25, n° 1, pp 35-61, 1983.

[27] HEDSTRÖM G.W., *Nonreflecting Boundary Conditions for Nonlinear Hyperbolic Systems*. J of Comp. Phys, vol 30, pp 222-237, 1979.

[28] HUANG K., *Statistical Mechanics*, J Wiley & Sons, New York, 1963.

[29] LAX P.D., *Hyperbolic Systems of Conservation Laws and the Mathematical Theory of Shock Waves*, CBMS Regional Conferences Series in Applied Maths, SIAM, Philadelphia, 1973.

[30] LIU T.P., *Initial-Boundary Value Problems for Gas Dynamics*, Arch. Rat. Mech. Anal, vol 64, pp 137-168, 1977.

[31] MAZET P.A., BOURDEL F., GREBORIO R.M., BOREE J., *Applications de la méthode variationnelle d'entropie à la résolution des équations d'Euler*. Internal Report, CERT, Toulouse, 1987.

[32] NISHIDA T., SMOLLER J., *Mixed Problems for Nonlinear Conservation Laws*, J. Diff. Equations, vol 23, n° 2, pp 244-269, 1977.

[33] OLIGER J., SUNDSTRÖM A., *Theoretical and Practical Aspects of Some Initial Boundary Value Problems in Fluid Dynamics*. SIAM J Appl. Math, vol 35, n° 3, pp 419-446, 1978.

[34] OSHER S., *Numerical Solution of Singular Perturbation Problems and Hyperbolic Systems of Conservation Laws*, in Math Studies n° 47 (Axelsson-Frank-Van der Sluis Eds), North Holland, Amsterdam, pp 179-205, 1981.

[35] OSHER S., SOLOMON F., *Upwind Difference Schemes for Hyperbolic Systems of Conservation Laws*, Math of Comp, vol 38, n° 158, pp 339-374, 1982.

[36] OSHER S., *Riemann Solvers, the Entropy Condition, and Difference Approximations*, SIAM J. Numer. Anal., vol 21, n° 2, pp 217-235, 1984.

[37] RAI M., CHAKRAVARTHY S., *An Implicit Form for the Osher Upwind Scheme*, AIAA J., vol 24, n° 5, pp 735-743, 1986.

[38] RIZZI A., *Computation of Rotational Transonic Flow*, in Numerical Methods for the Computation of Inviscid Transonic Flows with Shock Waves (Rizzi-Viviand Eds), Vieweg & Sohn, Braunschweig, pp 153-161, 1981.

[39] ROE P.L., *Approximate Riemann Solvers, Parameter Vectors, and Difference Schemes*, J. of Comp. Phys., vol 43, pp 357-372, 1981.

[40] SHUBIN G., STEPHENS A., GLAZ H., *Steady Shock Tracking and Newton's Method Applied to One-Dimensional Duct Flow*, J. of Comp. Phys., vol 39, pp 364-374, 1981.

[41] SMOLLER J., *Shock-Waves and Reaction-Diffusion Equations*, Springer-Verlag, Berlin, 1983.

[42] SOD G.A, *A survey of Several Finite Difference Methods for Systems of Nonlinear Hyperbolic Conservation Laws*, J. of Comp. Phys., vol 27, pp 1-31, 1978.

[43] STEGER J., WARMING R., *Flux-vector Splitting of the Inviscid Gas Dynamics Equations with Applications to Finite-Difference Methods*, J. of Comp. Phys., vol 40, pp 263-293, 1981.

[44] VAN LEER B., *Flux-vector Splitting for the Euler Equations*, in Lecture Notes in Physics n° 170 (Krause Ed), Springer, Berlin, pp 507-512, 1982.

[45] VAN LEER B., *On the Relation between the Upwind-Differencing Schemes of Godunov, Engquist-Osher and Ree*, SIAM J. Stat. Comput., vol 5, n° 1, pp 1-20, 1984.

[46] VILA J.P., *Sur la théorie et l'approximation numérique de problèmes hyperboliques non linéaires. Application aux équations de Saint-Venant et à la modélisation des avalanches de neige dense*, Thesis, Paris 6 Univ, 1986.

[47] VILA J.P., *Simplified Godunov Schemes for 2 × 2 Systems of Conservation Laws*, SIAM J. Numer. Anal., vol 23, n° 6, pp 1173-1192, 1986.

[48] VIVIAND H., VEUILLOT J.P., *Méthodes Pseudo-instationnaires pour le Calcul d'Ecoulements Transsoniques*, ONERA T.P. n° 1978-4, 1978.

[49] WHITHAM G.B., *On the Propagation of Weak Shock Waves*, J. of Fluid Mech, vol 1, pp 290-318, 1956.

[50] YEE H., BEAM R., WARMING R., *Boundary Approximations for Implicit Schemes for One-Dimensional Inviscid Equations of Gasdynamics*, AIAA J., vol 20, n° 9, pp 1203-1211, 1982.